ELECTRON RADIATION DAMAGE OF (AlGa)As – GaAs SOLAR CELLS

R. Loo, G.S. Kamath, R. Knechtli

Hughes Research Laboratories
3011 Malibu Canyon Road
Malibu, CA 90265

October 1979

Contract 955062
Final Technical Report
For period 25 April 1978 through 24 April 1979

Prepared for:
JET PROPULSION LABORATORY
California Institute of Technology
Pasadena, CA 91103

HUGHES

HUGHES AIRCRAFT COMPANY
RESEARCH LABORATORIES

ELECTRON RADIATION DAMAGE OF (AlGa)As-GaAs SOLAR CELLS

FINAL TECHNICAL REPORT
Contract 955062
For period 25 April 1978 through 24 April 1979

OCTOBER 1979

Prepared by
Hughes Research Laboratories
3011 Malibu Canyon Road
Malibu, CA 90265

Prepared for
JET PROPULSION LABORATORY
California Institute of Technology
Pasadena, CA 91103

This work was performed for the Jet Propulsion Laboratory, California Institute of Technology sponsored by the National Aeronautics and Space Administration under Contract NAS7-100.

TABLE OF CONTENTS

SECTION		PAGE
	LIST OF ILLUSTRATIONS	5
	LIST OF TABLES	9
1	INTRODUCTION AND SUMMARY	13
2	PHOTOCURRENT-VOLTAGE CHARACTERISTICS	23
3	SPECTRAL RESPONSE	33
4	RADIATION ANNEALING EXPERIMENTS	43
5	CONCLUSION AND SUMMARY	53
	APPENDIX A	55
	APPENDIX B	67
	APPENDIX C	75

LIST OF ILLUSTRATIONS

FIGURE		PAGE
1	The baseline design of (AlGa)As-GaAs solar cell	14
2	(a) Effect of junction depth x_j on radiation hardness	17
	(b) The absolute power of the (AlGa)As-GaAs solar cells versus 1 meV electron irradiation fluence (JPL measurements)	18
3	(a) Isochronal thermal annealing experiment on the 1 meV radiation damaged (AlGa)As-GaAs solar cell (cell 2747)	20
	(b) Isothermal annealing experiment at 200°C on the 1 meV, 1 x 10^{15} e/cm^{-2} radiation-damaged (AlGa)As-GaAs solar cell (cell 2401)	21
4	HRL's solar simulator spectrum in relation to the AM0 spectrum	28
5	(a) Photo I-V characteristcis of (AlGa)As-GaAs solar cell with 1 μm junction depth	30
	(b) Photo I-V characteristics of (AlGa)As-GaAs solar cell with 0.5-μm junction depth	30
	(c) Photo I-V characteristics of (AlGa)As-GaAs solar cell with 0.3-μm junction depth	30
6	(AlGa)As-GaAs solar cell spectral response (cell 2401, junction depth x_j = 0.5 μm) before and after 1-MeV electron irradiation (fluence = 1 x 10^{16} e cm^{-2})	34
7	(AlGa)As-GaAs solar cell spectral response (cell 2405, junction depth x_j = 0.5 μm) before and after 1-MeV electron irradiation (fluence = 1 x 10^{15} e cm^{-2})	35

FIGURE		PAGE
8	(AlGa)As-GaAs solar cell spectral response (cell 2373, junction depth x_j = 0.5 μm) before and after 1-MeV electron irradiation (fluence = 1 x 10^{15} e cm^{-2})	36
9	(AlGa)As-GaAs solar cell spectral response (cell 2403, junction depth x_j = 0.5 μm) before and after 1-MeV electron irradiation (fluence = 1 x 10^{15} e cm^{-2})	37
10	(AlGa)As-GaAs solar cell spectral response (cell 2747, junction depth x_j = 0.5 μm) before and after 1-MeV electron irradiation (fluence = 1 x 10^{16} e cm^{-2})	38
11	(AlGa)As-GaAs solar cell spectral response (cell 2796, junction depth x_j = 0.3 μm) before and after 1-MeV electron irradiation (fluence = 1 x 10^{16} e cm^{-2})	39
12	Spectral response after 1-MeV electron irradiation (1 x 10^{16} e cm^{-2}) for x_j = 0.3 μm and x_j = 0.5 μm (AlGa)As-GaAs solar cells	40
13	Typical temperature cycle for the thermal annealing experiment	44
14	(a) Photo I-V characteristics (cell 2401)	47
	(b) (AlGa)As-GaAs solar cell spectral response (cell 2401)	47
15	(a) Photo I-V characteristics (cell 2405)	48
	(b) (AlGa)As-GaAs solar cell spectral response (cell 2405)	48
16	(a) Photo I-V characteristics (cell 2373)	49
	(b) (AlGa)As-GaAs solar cell spectral response (cell 2373)	49
17	(a) Photo I-V characteristics (cell 2403)	50
	(b) (AlGa)As-GaAs solar cell spectral response (cell 2403)	50

FIGURE		PAGE
18	(a) Photo I-V characteristics (cell 2747).	51
	(b) (AlGa)As-GaAs solar cell spectral response (cell 2403)	51
19	(a) Photo I-V characteristics (cell 2796) . . .	52
	(b) (AlGa)As-GaAs solar cells spectral response (cell 2796)	52

LIST OF TABLES

TABLE		PAGE
1	Three Phases of (AlGa)As-GaAs Solar Cells Used for 1-MeV Electron Irradiation Studies	15
2	The Test Matrix for the (AlGa)As-GaAs Solar Cell Under 1-MeV Electron Irradiation	16
3	Critical Fluences for the 1-MeV Electron Radiation Damage on the (AlGa)As-GaAs Solar Cell as a Function of Junction Depth	19
4	HRL Measurements on (AlGa)As-GaAs Solar Cells (Phase 1 Cells) before and after 1-MeV Electron Irradiation	24
5	JPL Measurements on (AlGa)As-GaAs Solar Cells (Phase 1 Cells) before and after 1-MeV Electron Irradiation	24
6	HRL Measurements on (AlGa)As-GaAs Solar Cells (Phase 2 Cells) before and after 1-MeV Electron Irradiation	25
7	JPL Measurements on (AlGa)As-GaAs Solar Cells (Phase 2 Cells) before and after 1-MeV Electron Irradiation	25
8	HRL Measurements on (AlGa)As-GaAs Solar Cells (Phase 3 Cells) before and after 1-MeV Electron Irradiation	26
9	JPL Measurements on (AlGa)As-GaAs Solar Cell (Phase 3 Cells) before and after 1-MeV Electron Irradiation	26
10	HRL Measurements on (AlGa)As-GaAs Solar Cells after 1-MeV Electron Irradiation	27
11	Thermal Annealing Characteristics of 1-MeV Electron Radiation Damaged (AlGa)As-GaAs Solar Cells	45
12	Thermal Annealing Characteristics of 1 MeV Electron Radiation Damaged (AlGa)As-GaAs Solar Cells	46

ABSTRACT

Solar cells — 2 cm by 2 cm (AlGa)As-GaAs cells — were fabricated and then subjected (at JPL) to irradiation at normal incidence by electrons. The contract objective was to determine the influence of junction depth and n-type buffer layer doping level on the cell's resistance to radiation damage. Three sets of cells were used: (1) junction depth of 0.5 μm, a buffer layer doping level of $N_D = 1 \times 10^{17}$ cm^{-3}; (2) 0.3 μm junction depth, the same doping level; and (3) 0.3 μm junction depth, a doping density of the buffer layer of only 1×10^{16} cm^{-3}.

The present study shows that (1) a 0.3-μm-deep junction results in lower damage to the cells than does a 0.5-μm junction, and (2) lowering the n buffer layer doping density from 1×10^{17} cm^{-3} to 1×10^{16} cm^{-3} does not improve the radiation resistance of the cell. Rather, lowering the doping density decreases the solar cell's open-circuit voltage.

Some preliminary thermal annealing experiments in vacuum were performed on these (AlGa)As-GaAs solar cells damaged by 1-MeV electron irradiation. Results showed that cell performance can be expected to partially recover at 200°C with more rapid and complete recovery (in both I_{sc} and V_{oc}) occurring at higher temperature. For a 0.5-hr anneal at 400°C, 90% of the initial power is recovered. This report describes characteristics of the (AlGa)As-GaAs cells both before and after irradiation.

SECTION 1

INTRODUCTION AND SUMMARY

The purpose of this contract was to study the effect of high-energy electron irradiation on the performance of (AlGa)As-GaAs solar cells. This was part of a joint effort with Dr. Bruce Anspaugh of JPL to optimize the resistance of these cells to radiation damage and exploit them for near sun missions of interest to JPL. Specifically, the effects of junction depth and doping level on the cells' resistance to radiation damage were investigated under this contract, including measurements on cells whose junction depth was shallower than that of the cells studied in earlier investigations. Preliminary measurements on thermal annealing were also performed. Because of the limited level of effort available, this contract's effort was limited to irradiation with 1-MeV electrons.

The 1-MeV electron irradiation was performed at JPL using the dynamitron particle accelerator. The uniformity over the test plane was ±4% with no area of discontinuity. Fluxes and fluences were measured with a Faraday cup, the current of which was integrated to establish electron fluences and to automatically stop the irradiation at the desired fluence levels.

Figure 1 shows the (AlGa)As-GaAs solar cell structure used for this study. The n buffer layer was LPE grown on the n^+ GaAs substrate. The $(Al_xGa_{1-x})As$ window layer was also grown by LPE on the n buffer layer. Our window layer had an aluminum content $x > 0.90$, making the bandgap and hence the optical transmission as high as possible. The dopant was beryllium. During (AlGa)As window layer growth, a p-n homojunction was formed by Be diffusion from the (AlGa)As layer into the n buffer layer. The total diffused region, the distance x_j (Figure 1) sandwiched between the heterojunction and homojunction, is known as the junction depth.

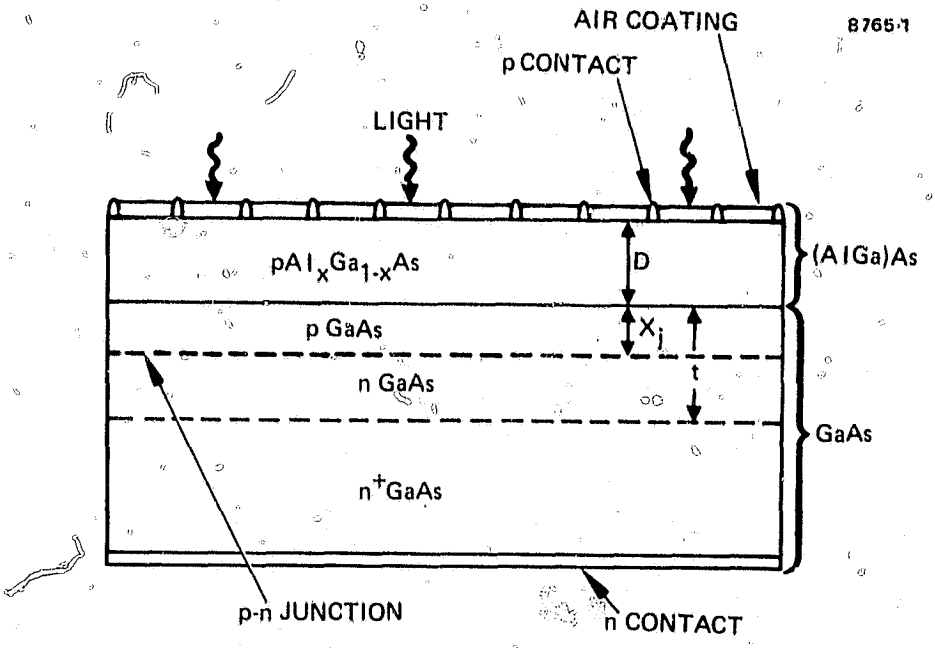

Figure 1. The baseline design of (AlGa)As-GaAs solar cell.

We made three sets of (AlGa)As-GaAs solar cells for 1-MeV electron radiation damage testing. Table 1 gives the cell parameters for the cells made for each phase of this contract. Table 10 gives the cell parameters for cells made prior to this contract and used for comparison purposes further on. The phase 1 cells were LPE grown at 790°C for 2 min, and the measured junction depths (x_j) were between 0.45 μm and 0.5 μm. The phase 2 cells were LPE grown at 700°C for 4 min. This produced a junction depth x_j of 0.3 μm. The objective of this phase of the program was to verify our theoretical prediction that the optimum junction depth for minimum radiation damage is smaller than 0.5 μm. (In previous projects, we had already demonstrated a major improvement* by going from $x_j \simeq 1.0$ μm to $x_j \simeq 0.5$ μm, while our theoretical calculations lead us to expect the optimum to be in the vicinity of $x_j \simeq 0.2$ μm.) The phase 3 cells were also grown at 700°C for 4 min, and their cell structure is identical to the phase 2 cells, except that the doping density in the n

*See Appendix A, Figure A-7.

buffer layer is 1×10^{16} cm^{-3} instead of 1×10^{17} cm^{-3}. Table 2 gives the test matrix for the 1-MeV electron irradiation of these solar cells. Our phase 2 and 3 cells have thicker window layers than do the phase 1 cells because the LPE growth schedule was designed to yield a junction depth of 0.3 μm. The growth schedule had not yet been fully optimized to provide accurate control of all the structural parameters of the cell. The emphasis on the junction depth reflects our feeling that the junction depth is the most important and sensitive parameter controlling the cell's radiation resistance. This emphasis evolved from results that we had obtained prior to this contract with cells that had junction depths of 1.0 μm and 0.5 μm (see Section 2 and Table 10). After electron irradiation, the phase 2 and 3 cells with the shallowest junction depths did in fact have the greatest radiation resistance (see Figure 2(b)).

Table 1. Three Phases of (AlGa)As-GaAs Solar Cells Used for 1-MeV Electron Irradiation Studies

Phase 1		
Window layer thickness (D)	=	0.5 μm
Junction depth (x_j)	=	0.5 μm
Buffer layer doping density (N_D)	=	1×10^{17} cm^{-3}
Phase 2		
Window layer thickness (D)	=	1.1 μm
Junction depth (x_j)	=	0.3 μm
Buffer layer doping density (N_D)	=	1×10^{17} cm^{-3}
Phase 3		
Window layer thickness (D)	=	1.1 μm
Junction depth (x_j)	=	0.3 μm
Buffer layer doping density (N_D)	=	1×10^{16} cm^{-3}

6664

Table 2. The Test Matrix for the (AlGa)As-GaAs Solar Cell Under 1-MeV Electron Irradiation

Cells	1-MeV Electron Irradiation				(AlGa)As-GaAs Solar Cell Numbers
	Temperature, °C	Time	Flux, e cm^{-2} sec^{-1}	Fluence, e cm^{-2}	
Phase 1	28	13 hr	2×10^{10}	1×10^{15}	2401, 2405
	126	13 hr	2×10^{10}	1×10^{15}	2373, 2403
Phase 2	28		1×10^{12}	1×10^{15}	2747, 2770
	28	92 min	1×10^{12}	1×10^{16}	2747, 2770
Phase 3	28		1×10^{12}	1×10^{15}	2793, 2796
	28	92 min	1×10^{12}	1×10^{16}	2793, 2796

6664

Figure 2(a) shows P_I/P_o as a function of 1-MeV electron irradiation fluence for 0.3 μm, 0.5 μm, and 1.0 μm junction depth cells. P_o and P_I are the power output (P_{max}) from the cell before and after irradiation, respectively. The 1.0 μm and some of the 0.5 μm junction depth cells had been studied prior to this contract, under a previous IR&D program. (They had also been irradiated at JPL.) Data from these prior cells is used here to compare the effect of junction depth X_j on radiation hardness over the extended range from 1.0 μm down to 0.3 μm. We feel that using the P_I/P_o ratio enables us to compare the degradation of the cell efficiency as a function of junction depth. We realize that, for space application, the absolute power at the end of life is more significant for calculating panel requirements. However, we believe that the cell's structure for any particular junction depth can be optimized to yield the maximum absolute efficiency up to 18 to 20% AMO. This belief is based on our past experience in increasing the cell efficiency at junction depths of 0.8 and 0.5 μm. The gains in radiation resistance from decreased junction depth should therefore, lead to the highest performance cells in space flight, and we will continue to develop shallower junction

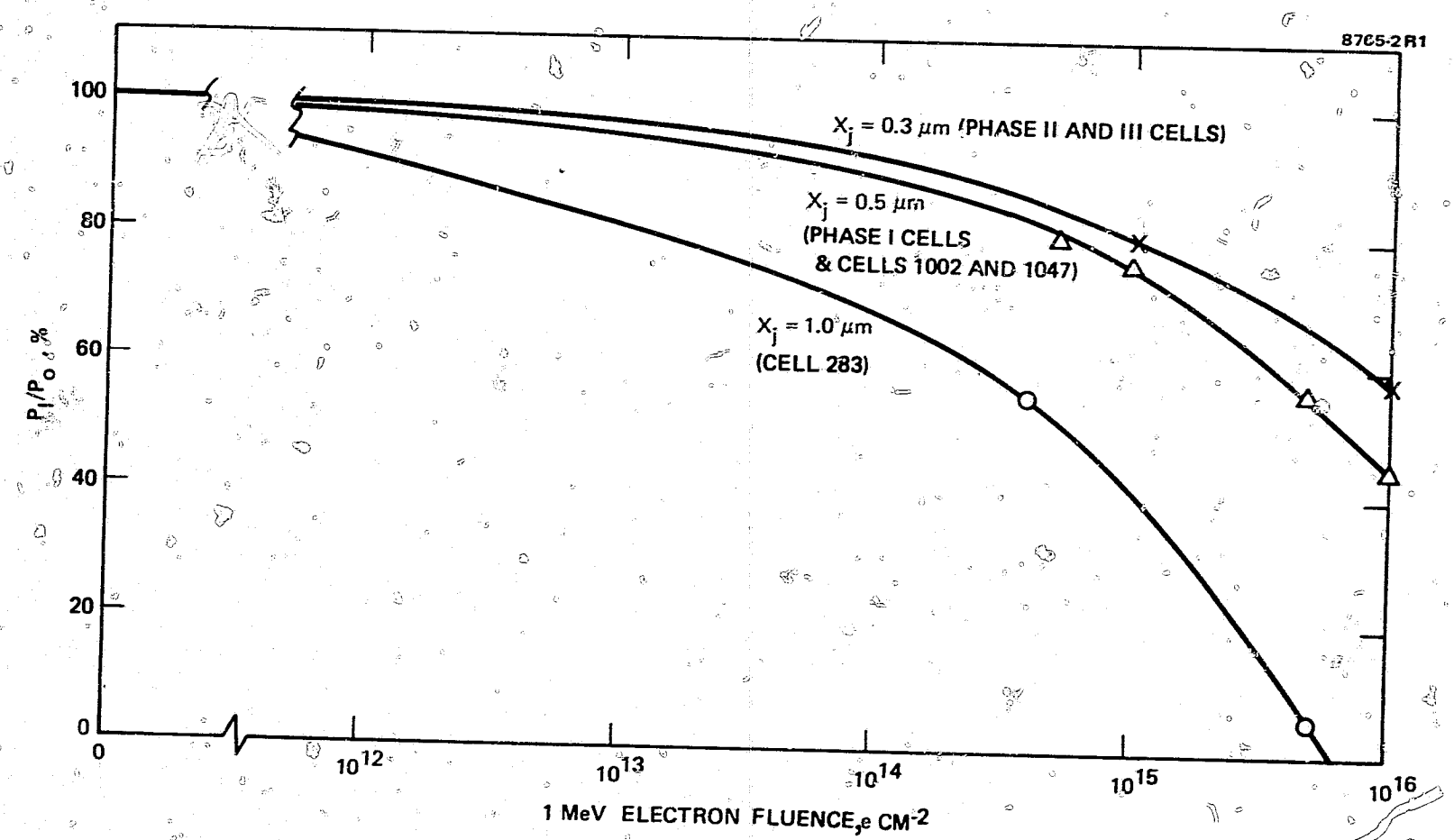

Figure 2(a). Effect of junction depth x_j on radiation hardness. (P_o = maximum power before irradiation, P_I = maximum power after irradiation.)

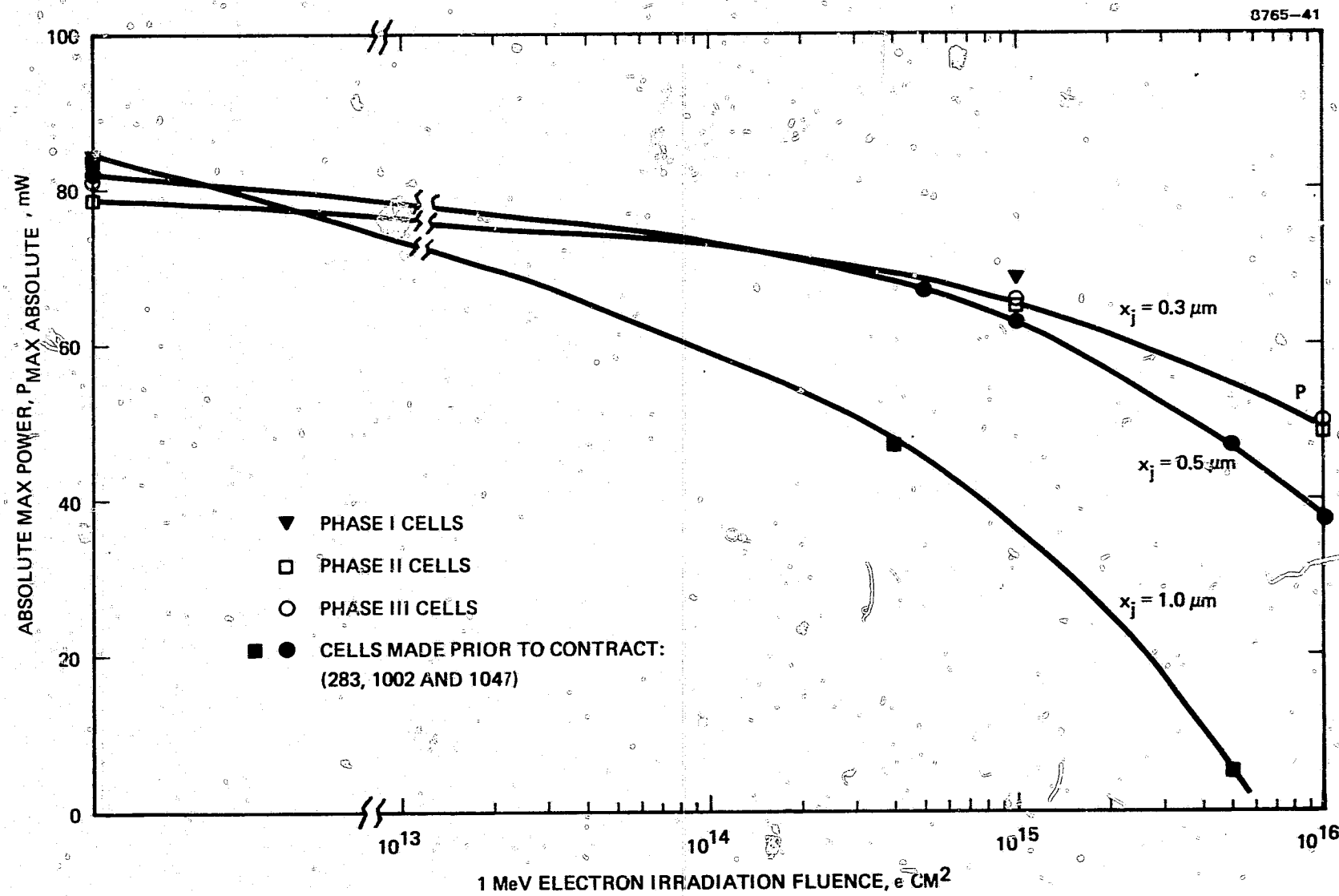

Figure 2(b). The absolute maximum power of the (AlGa)As-GaAs solar cells versus 1 MeV electron irradiation fluence (JPL measurements).

cells to meet this requirement. Figure 2(b) shows the absolute power P_{max} for the Phase 1, 2, and 3 cells as well as our previous data on deeper junction cells. The influence of the irradiation on cell performance can, however, be seen more easily from the results in Figure 2(a) than from those in Figure 2(b), which indicates that the best resistance to radiation damage is indeed obtained with the shallowest junction cells (0.3-μm junction depth). Table 3 gives the critical fluence as a function of junction depth. The critical fluence is defined as the fluence level at which the maximum output power of the solar cell is reduced by 25% under 1-MeV electron irradiation ($P_I/P_o = 0.75$).

Some preliminary thermal annealing experiments in vacuum on the radiation-damaged (AlGa)As-GaAs solar cells were performed at HRL (see Section 4 for experimental details). The damage GaAs solar cells were found to recover most of their efficiency rather rapidly when annealed at temperatures above 200°C. Figure 3 summarizes these results by showing the effect of thermal annealing as functions of annealing temperature and time. The data in Figure 3(b) indicate that at least partial recovery of cell performance can be expected at 200°C. Figure 3(a) shows that, above 200°C, the annealing leads to recovery of both I_{sc} and V_{oc} at a more rapid rate with increasing temperature, eventually leading to greater than 90% recovery of the preirradiation power levels. In addition, the GaAs cells tested were not damaged by either repeated temperature cycling (from room temperature and up) or by annealing at 400°C for 1/2 hr.

Table 3. Critical Fluences for the 1-MeV Electron Radiation Damage on the (AlGa)As-GaAs Solar Cell as a Function of Junction Depth

(AlGa)As-GaAs Solar Cell Junction Depth, cm	Critical Fluence, e cm^{-2}
1.0	3×10^{13}
0.5	1×10^{15}
0.3	2×10^{15}

6664

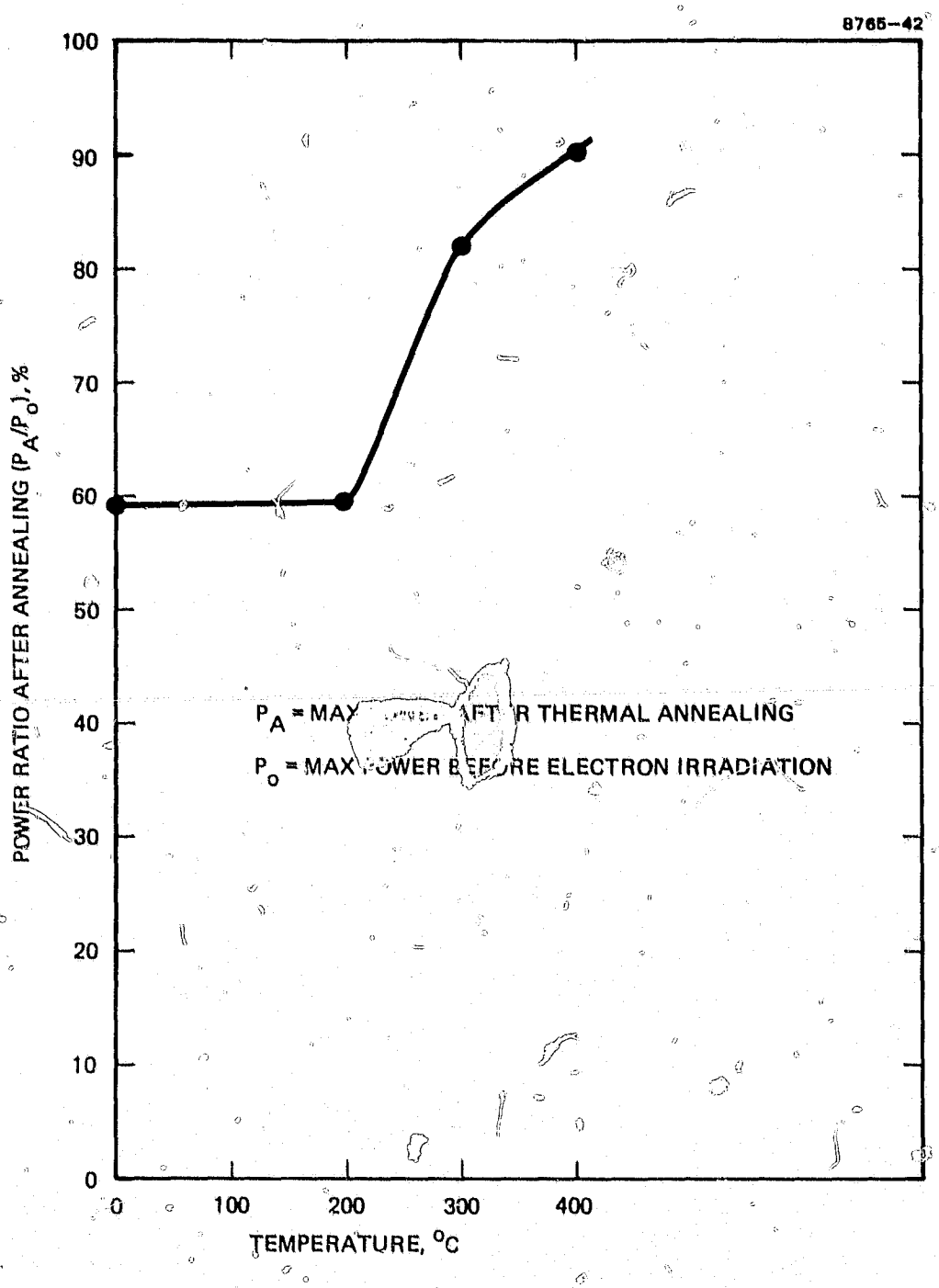

Figure 3(a). Isochronal thermal annealing experiment on the 1 MeV radiation damaged (AlGa)As-GaAs solar cell (cell 2747). (Total annealing times = 0.5 hr at each temperature.)

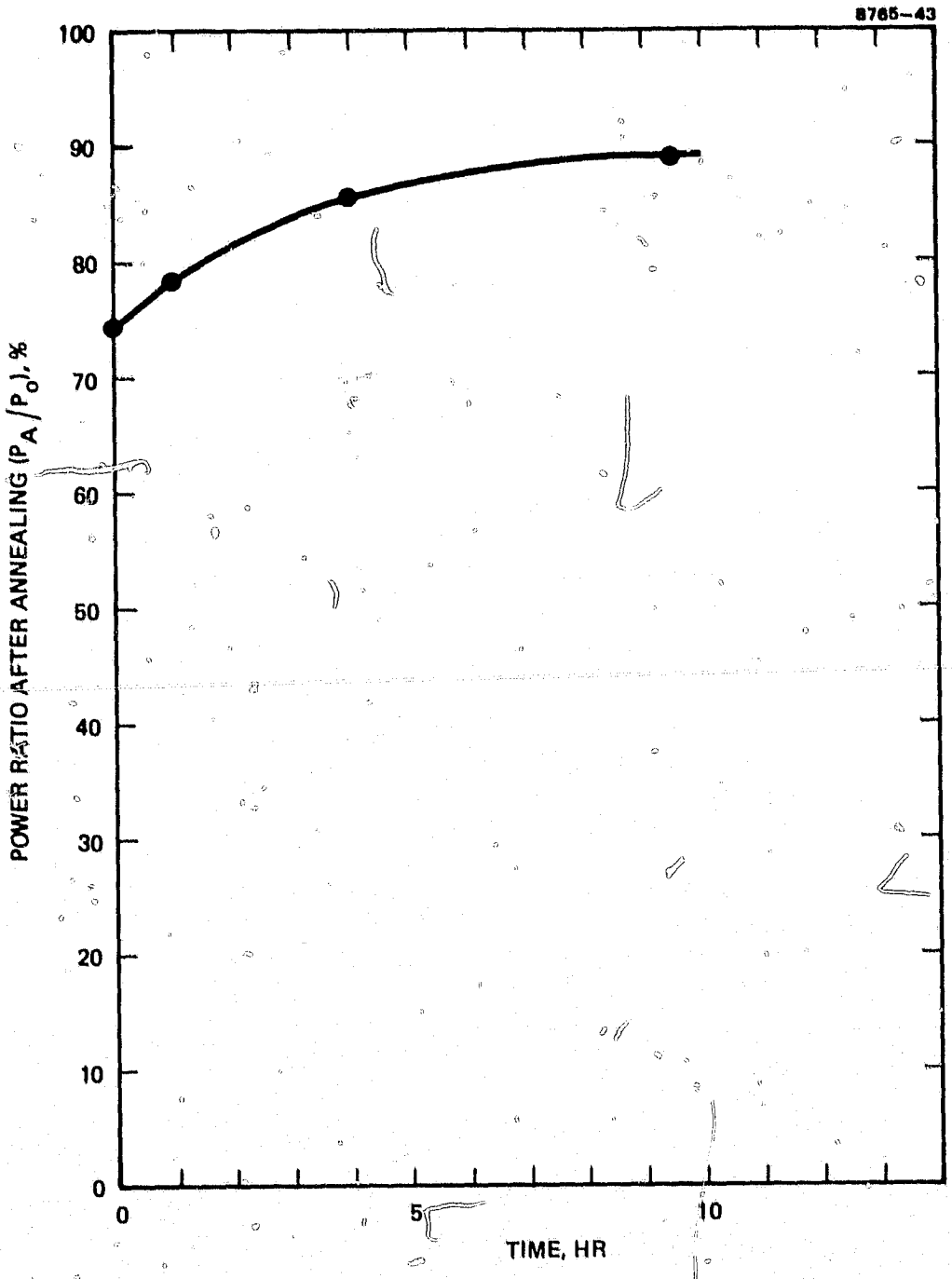

Figure 3(b). Isothermal annealing experiment at 200°C on the 1 MeV, 1 x 10^{15} e cm^{-2} radiation-damaged (AlGa) As-GaAs solar cell (cell 2401).

In summary, we confirmed the importance of decreasing the junction depth to below 0.5 μm to minimize radiation damage. We also confirmed that rapid thermal annealing sufficient to eliminate most of the radiation damage can occur at annealing temperatures as low as 200°C. The detailed data leading to these conclusions is given and discussed in the balance of this report.

SECTION 2

PHOTOCURRENT-VOLTAGE CHARACTERISTICS

Both the HRL and JPL solar simulators were used in measuring the photo I-V characteristics of the solar cells. The intensity of the HRL solar simulator was standardized against our high-altitude flight standard GaAs solar cells; these cells were also cross checked by the Spectrolab Mark III solar simulator. The HRL test block temperature, on which the cells were held during the measurement, is controlled by cooling water and is kept at 22°C. The JPL test block temperature is kept at 28°C. This temperature difference accounts for the slightly higher open-circuit voltage observed in the measurements made at HRL. (The effect of temperature on (AlGa)As solar cells is discussed in Appendix C.)

Appendix B shows the I-V characteristics for the (AlGa)As-GaAs solar cells before and after the irradiation. Figures B-1 through B-6 show the I-V curves as measured by the HRL solar simulator. Figures B-7 through B-12 show comparable results obtained with the JPL solar simulator. Tables 4 through 10 give the following individual cell characteristics: short-circuit current (I_{sc}), open-circuit voltage (V_{oc}), fill factor (FF), and maximum power conversion efficiency (η). Table 10 gives the electrical characteristics of cells 283, 1002, and 1047 before and after the electron irradiation (these cells had been made prior to the present contract). Both the junction depth and window layer thickness are specified in Table 10. Although cell 283 has the same window layer thickness as does our phase 3 cells, its junction depth is much greater (1.0 μm) than that of the phase 3 cells (0.3 μm).

Results of measurements made at both HRL and at JPL are given in Tables 4 through 9. The slightly higher values of the cell's open-circuit voltage in the HRL measurement are attributed to the temperature differences between the test blocks (as mentioned before). Both the HRL and JPL measurements of short-circuit current were in good agreement before the irradiation. However, after irradiation, values of

Table 4. HRL Measurements on (AlGa)As-GaAs Solar Cells (Phase 1 Cells) before and after 1-MeV Electron Irradiation

Cell Number	Irradiation Temperature, °C	Fluence, e cm^{-2}	I_{sc}, mA	V_{oc}, V	FF	P_m, mW	η, %
2401	28	0	111.5	0.99	0.789	87.1	16.1
		1×10^{15}	90	0.90	0.815	66	12.2
2405	28	0	110	1.01	0.773	85.9	15.9
		1×10^{15}	88.5	0.90	0.80	64	11.8
2373	126	0	112	1.0	0.774	86.7	16.0
		1×10^{15}	88.5	0.90	0.773	61.6	11.4
2403	126	0	111	1.0	0.774	85.9	15.9
		1×10^{15}	90	0.90	0.799	64.7	12.0

6664

Table 5. JPL Measurements on (AlGa)As-GaAs Solar Cells (Phase 1 Cells) before and after 1-MeV Electron Irradiation

Cell Number	Irradiation Temperature, °C	Fluence, e cm^{-2}	I_{sc}, mA	V_{oc}, V	FF	P_m, mW	η, %
2401	28	0	111.2	0.985	0.787	86.2	15.9
		1×10^{15}	97.1	0.899	0.806	70.4	13.0
2405	28	0	110.7	0.991	0.768	84.2	15.6
		1×10^{15}	95.6	0.897	0.80	68.4	12.6
2373	126	0	109.7	0.965	0.747	79.1	14.6
		1×10^{15}	95	0.891	0.784	66.4	12.3
2403	126	0	110.9	0.983	0.773	84.3	15.6
		1×10^{15}	96.2	0.895	0.799	68.8	12.7

6664

Table 6. HRL Measurements on (AlGa)As-GaAs Solar Cells (Phase 2 Cells) before and after 1-MeV Electron Irradiation

Cell Number	Irradiation Temperature, °C	Fluence, e cm-2	I_{sc}, mA	V_{oc}, V	FF	P_m, mW	η, %
2747	28	0	105	0.98	0.77	79.3	14.6
		1×10^{16}	74	0.035	0.759	46.9	8.7
2770	28	0	104.1	0.971	0.784	79.3	14.7
		1×10^{16}	73	0.835	0.753	46	8.5

6664

Table 7. JPL Measurements on (AlGa)As-GaAs Solar Cells (Phase 2 Cells) before and after 1-MeV Electron Irradiation

Cell Number	Irradiation Temperature, °C	Fluence, e cm-2	I_{sc}, mA	V_{oc}, V	FF	P_m, mW	η, %
2747	28	0	105.4	0.973	0.76	78	14.4
		1×10^{15}	92.2	0.896	0.778	64.3	11.9
		1×10^{16}	77.5	0.820	0.766	48.7	9.0
2770	28	0	104.1	0.971	0.785	79.3	14.7
		1×10^{15}	89.9	0.894	0.791	63.6	11.8
		1×10^{16}	77	0.820	0.765	48.3	8.9

6664

Table 8. HRL Measurements on (AlGa)As-GaAs Solar Cells (Phase 3 Cells) before and after 1-MeV Electron Irradiation

Cell Number	Irradiation Temperature, °C	Fluence, e cm-2	I_{sc}, mA	V_{oc}, V	FF	P_m, mW	η, %
2793	28	0	107.5	0.97	0.80	83.7	15.5
		1×10^{16}	81	0.815	0.757	50	9.2
2796	28	0	103.5	0.974	0.81	81.2	15.0
		1×10^{16}	78	0.796	0.77	49.3	9.1

6664

Table 9. JPL Measurements on (AlGa)As-GaAs Solar Cell (Phase 3 Cells) before and after 1-MeV Electron Irradiation

Cell Number	Irradiation Temperature, °C	Fluence, e cm-2	I_{sc}, MA	V_{oc}, V	FF	P_m, mW	η, %
2793	28	0	106.5	0.956	0.799	81.4	15.0
		1×10^{15}	95.3	0.881	0.798	67.0	12.4
		1×10^{16}	83.3	0.798	0.762	50.7	9.4
2796	28	0	103.4	0.957	0.811	80.3	14.8
		1×10^{15}	92.2	0.880	0.796	64.6	11.9
		1×10^{16}	80.4	0.796	0.772	49.4	9.1

6664

short-circuit current measured at HRL were consistently lower than those measured at JPL. This discrepancy has been shown to result from the difference between the light spectra of the two solar simulators. Figure 4 shows the spectrum of the HRL solar simulator in relation to the AM0 spectrum. Figure 4 clearly shows that the HRL solar simulator is richer than the AM0 in the long-wavelength spectrum and poorer in the short-wavelength region. Thus, we would expect the GaAs solar cell to yield less current after irradiation when measured by the HRL solar simulator than when measured with the JPL simulator, the latter being more closely matched to the AM0's spectrum.

Table 10. HRL Measurements on (AlGa)As-GaAs Solar Cells after 1-MeV Electron Irradiation

Cell Number	Fluence, e cm^{-2}	I_{sc}, mA	V_{oc}, V	FF	P_m, mW	Efficiency, %	Junction Depth (x_j), μm	(AlGa)As Thickness, μm
283	0	106.3	0.91	0.81	78.7	14.5	1.0	1.0
	4×10^{14}	93	0.87	0.80	64.8	12.0		
	5×10^{15}	44	0.74	0.78	25.2	4.7		
1047	0	112	0.99	0.74	82	15.2	0.5	0.5
	1×10^{15}	85	0.91	0.78	60.4	11.2		
1002	0	108	1.0	0.76	82.2	15.2	0.5	0.5
	1×10^{16}	56	0.84	0.77	36.0	6.6		

6664

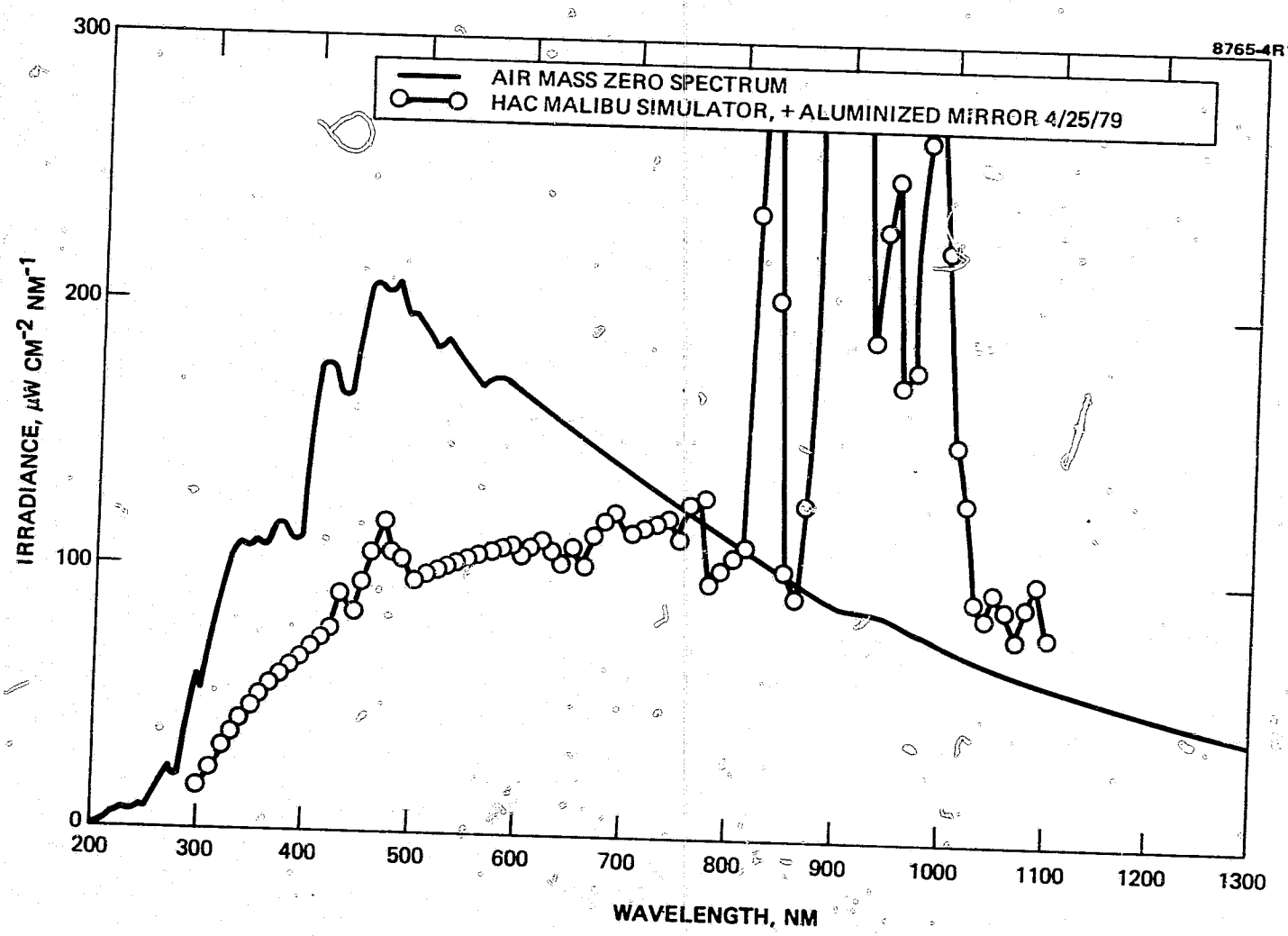

Figure 4. HRL's solar simulator spectrum in relation to the AM0 spectrum.

Figure 5 shows typical measured photo I-V characteristics before and after electron irradiation for our GaAs solar cells with junction depths of 0.3 μm (phase II and III cells) 0.5 μm, (cell 1002), and 1.0 μm (cell 283). The results clearly demonstrate that the difference in window layer thickness does not play an important role in radiation resistance, the junction depth is a sensitive parameter in determining radiation resistance, and the shallow junction solar cells show more irradiation resistance than do the deep junction cells, even down to a junction depth of 0.3 μm. Further reduction in junction depth to less than 0.3 μm should lead to even more radiation hardened GaAs solar cells, the optimum junction depth being estimated to be about 0.2 μm.

The doping density in the n base region does not play an important role in further increasing the radiation resistance of the cells. Tables 6 through 9 show the data on the phase 2 and 3 cells. On the contrary, the open-circuit voltage decreases as the doping density is reduced to 1×10^{16} cm^{-3}. The results would suggest that lower doping density in the base n layer is not desirable since it may lead to a lower beginning-of-life efficiency becuase the lower open-circuit voltage is not offset by an increase in radiation resistance. Such an improvement might have been hoped for as a result of the increased minority-carrier lifetime in the purer n-type material.

To investigate the effect of electron irradiation flux rate and irradiation temperature on the radiation resistance of GaAs solar cells, we irradiated two phase 1 cells at 126°C and two other phase 1 cells at room temperature (see Table 2). All these cells were subjected to a relatively low radiation flux rate 2×10^{10} e cm^{-2} sec^{-1} (13.5 hr of irradiation time to reach a fluence of 1×10^{15} e cm^{-2}). These results were compared with our previous radiation damage data on GaAs cells with 0.5 μm junction depth; these cells had been irradiated at a flux rate of 1×10^{12} e cm^{-2} sec^{-1}. The phase 1 cells, which were irradiated at room temperature, were also soaked in vacuum at 126°C for 13.5 hr to compare them with the cells irradiated at 126°C.

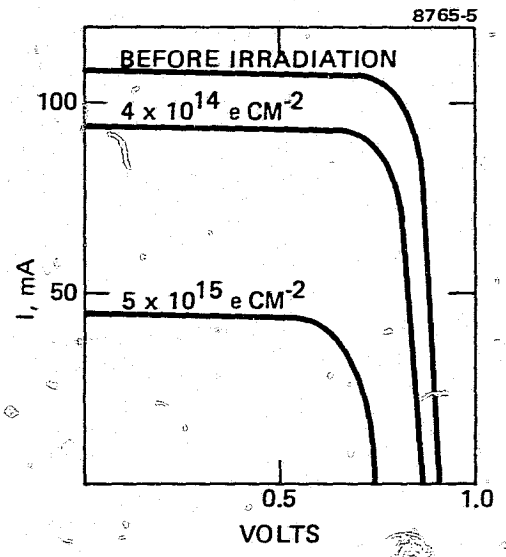

Figure 5(a).
Photo I-V characteristics of (AlGa)As-GaAs solar cell with 1-μm junction depth. Cell No. 283.

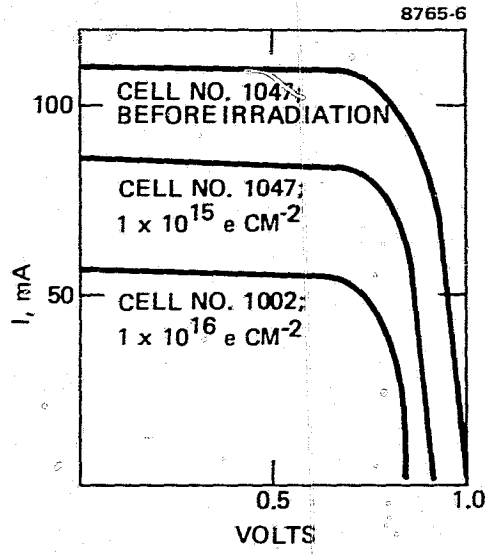

Figure 5(b).
Photo I-V characteristics of (AlGa)As-GaAs solar cell with 0.5-μm junction depth. Cell No. 1002.

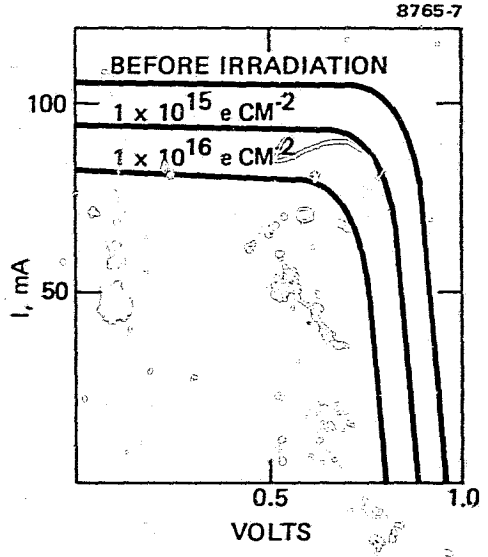

Figure 5(c).
Photo I-V characteristics of (AlGa)As-GaAs solar cell with 0.3-μm junction depth. Cell No. 2793.

The results show that neither the flux rate nor the irradiation temperature affects the radiation resistance characteristics of the cells. A temperature of 126°C is apparently too low to prevent damage produced by electron irradiation (see Section 5).

This result leads to several interesting conclusions:

- Junction depth is an important parameter in determining the radiation resistance of GaAs solar cells. Also, the study further confirms our shallow junction model and emphasizes the importance of keeping the junction depth shallow (≤0.3 μm) to minimize radiation damage in GaAs solar cells.
- Decreasing the flux rate to as low as 2×10^{10} e cm^{-2} sec^{-1} does not improve the radiation resistance of the cells
- An irradiation temperature of 126°C is not high enough to decrease the radiation damage to the GaAs solar cells.
- Lowering the buffer layer doping density to 1×10^{16} cm^{-3} does not seem to improve the cells' radiation resistance. It does, however, reduce the open-circuit voltage V_{oc} for the cell.

SECTION 3

SPECTRAL RESPONSE

Spectral response is measured at HRL using a Bausch and Lomb grating monochromator and a chopped tungsten light. The cell short-circuit current is measured with a PAR 124 lock-in amplifier with the incident radiation calibrated by a UDT silicon photodiode. The responsivity of the cell at each wavelength is the ratio of the short-circuit current to the incident power density. The conversion of responsivity to quantum efficiency is then accomplished by normalizing responsivity to the photon energy at each specific wavelength.

Figures 6 to 11 show the spectral response of the (AlGa)As-GaAs solar cells before and after 1-MeV electron irradiation.* (Cells 2373, 2401, 2403, and 2405 were irradiated at 1×10^{15} e cm^{-2}, and cells 2747 and 2796 were irradiated at 1×10^{16} e cm^{-2}). Figure 12 compares the spectral response of cells with 0.3- and 0.5-μm junction depths after radiation damage. The spectral response data of Figures 6 through 12 shows that, for cells with junctions shallower than 0.5 μm, the short-wavelength region is less sensitive to electron irradiation than the long-wavelength region. This is because, at short wavelengths, the absorption constants are large, the light is absorbed close to the surface, and the generated minority carriers then have to travel to the junction. If the electron diffusion length is longer than the junction depth, then the shallower the junction the less the loss due to recombinations. However, when the electron diffusion length in the p region becomes comparable to or less than the junction depth (deeper junction cells), the spectral response is substantially affected because of recombination losses.

*It should be noted that the difference in the data shown in Figures 6 through 9 on cells with identical design parameters results from the limited accuracy of our measurement and fabrication techniques. The fact the no radiation damage is apparent in Figure 9 for $\lambda < 0.55$ μm should not be given additional significance.

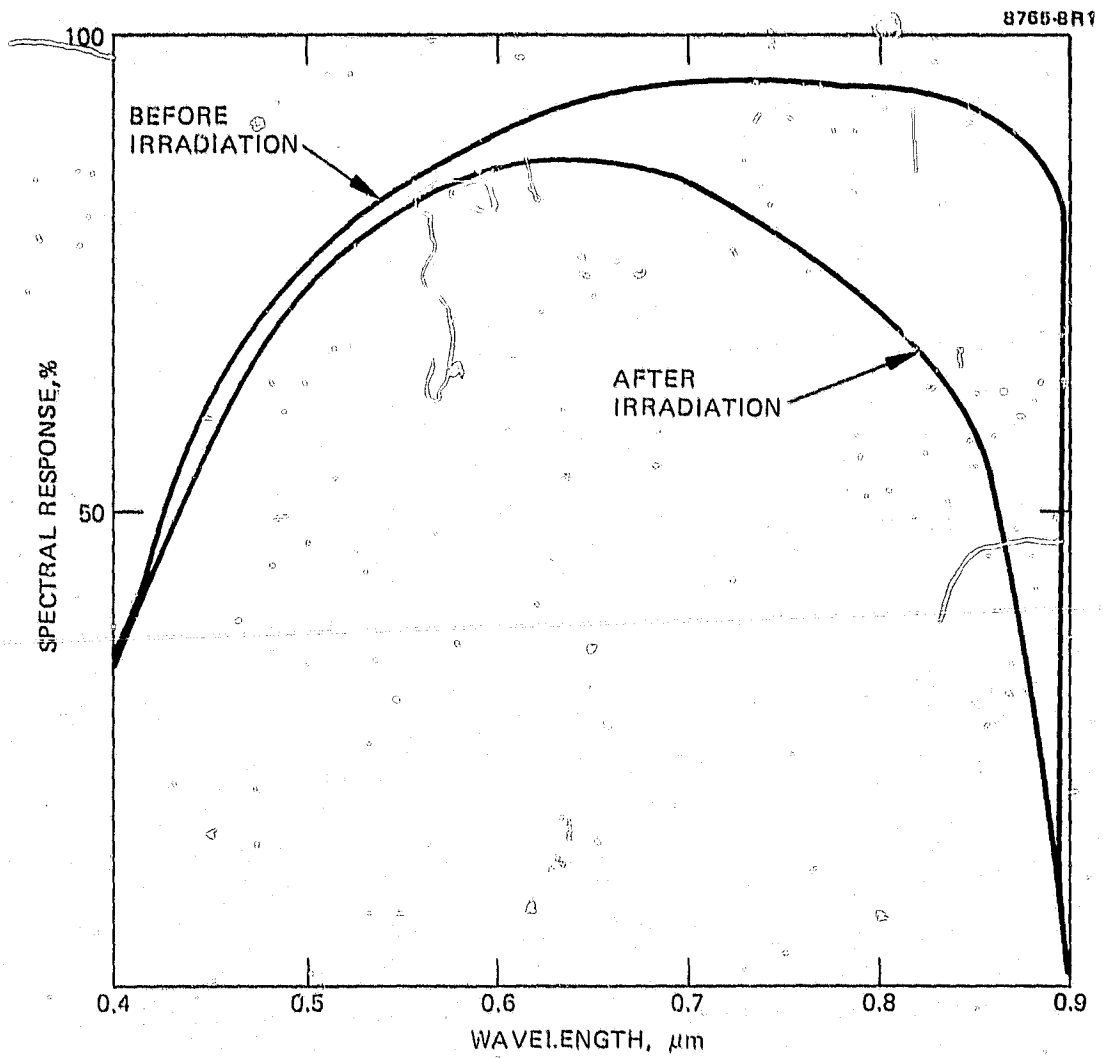

Figure 6. (AlGa)As-GaAs solar cell spectral response (cell 2401, junction depth x_j = 0.5 μm) before and after 1-MeV electron irradiation (fluence = 1 x 10^{16} e cm^{-2}).

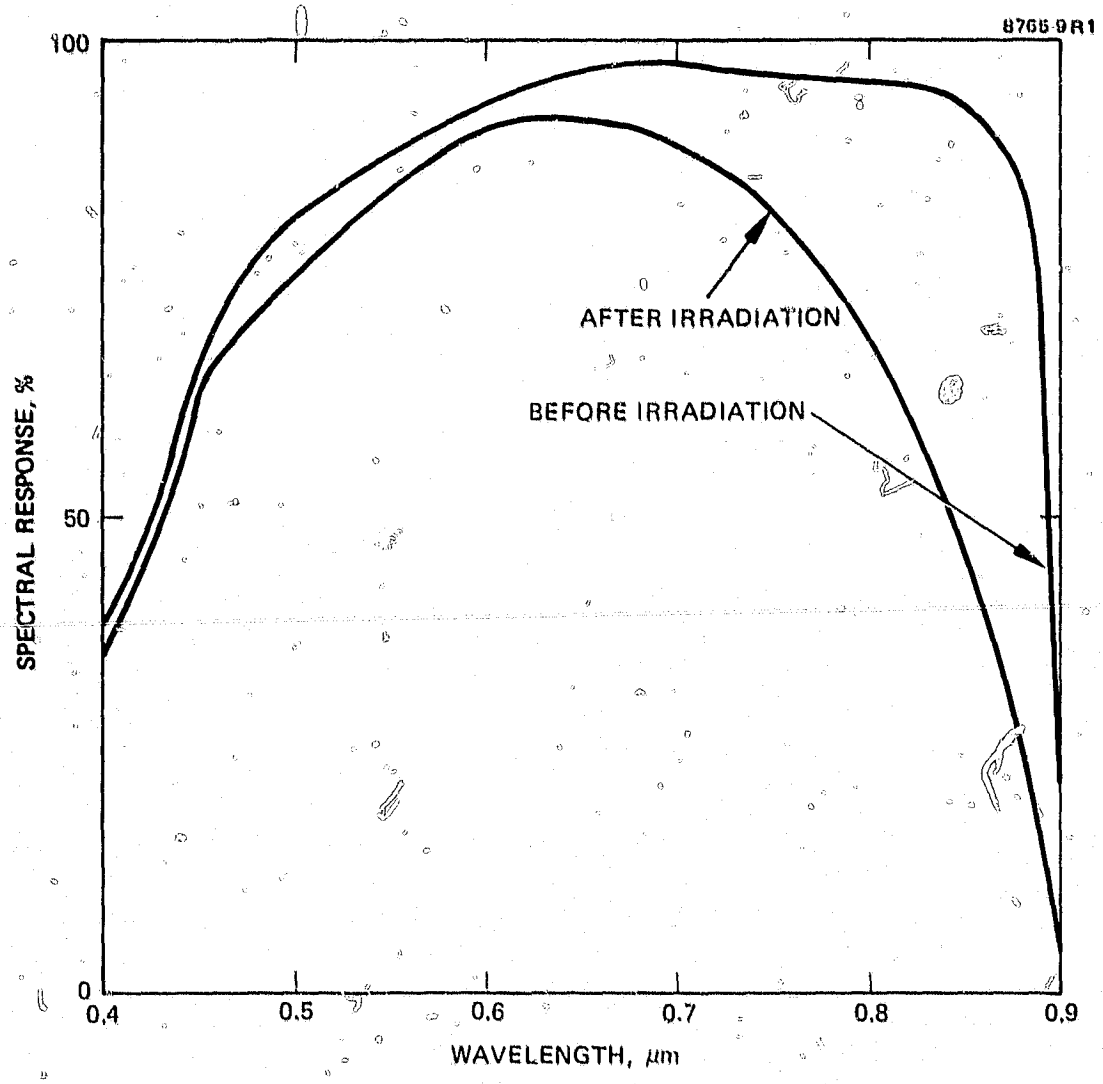

Figure 7. (AlGa)As-GaAs solar cell spectral response (cell 2405, junction depth x_j = 0.5 μm) before and after 1-MeV electron irradiation (fluence = 1 x 10^{15} e cm^{-2}).

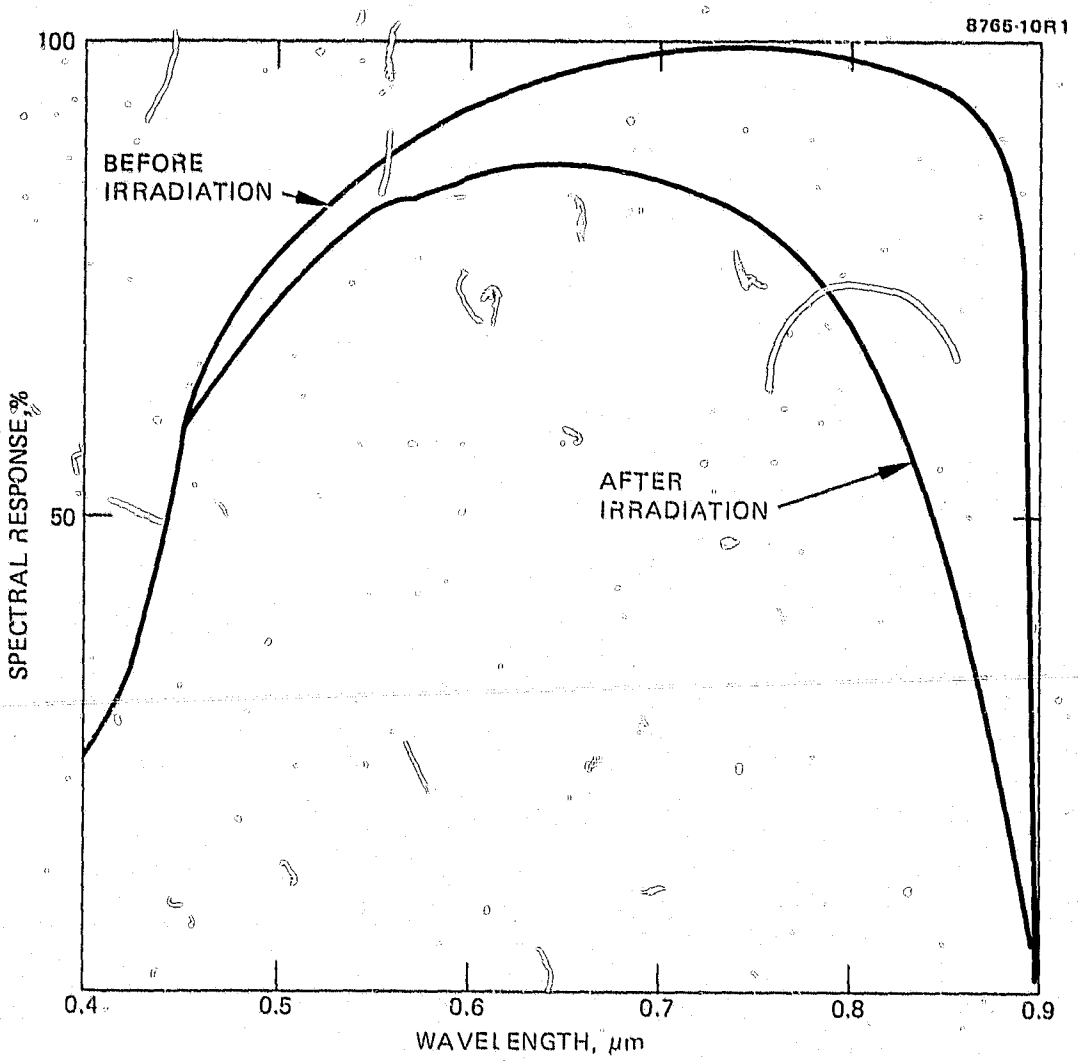

Figure 8. (AlGa)As-GaAs solar cell spectral response (cell 2373, junction depth x_j = 0.5 μm) before and after 1-MeV electron irradiation (fluence = 1×10^{15} e cm^{-2}).

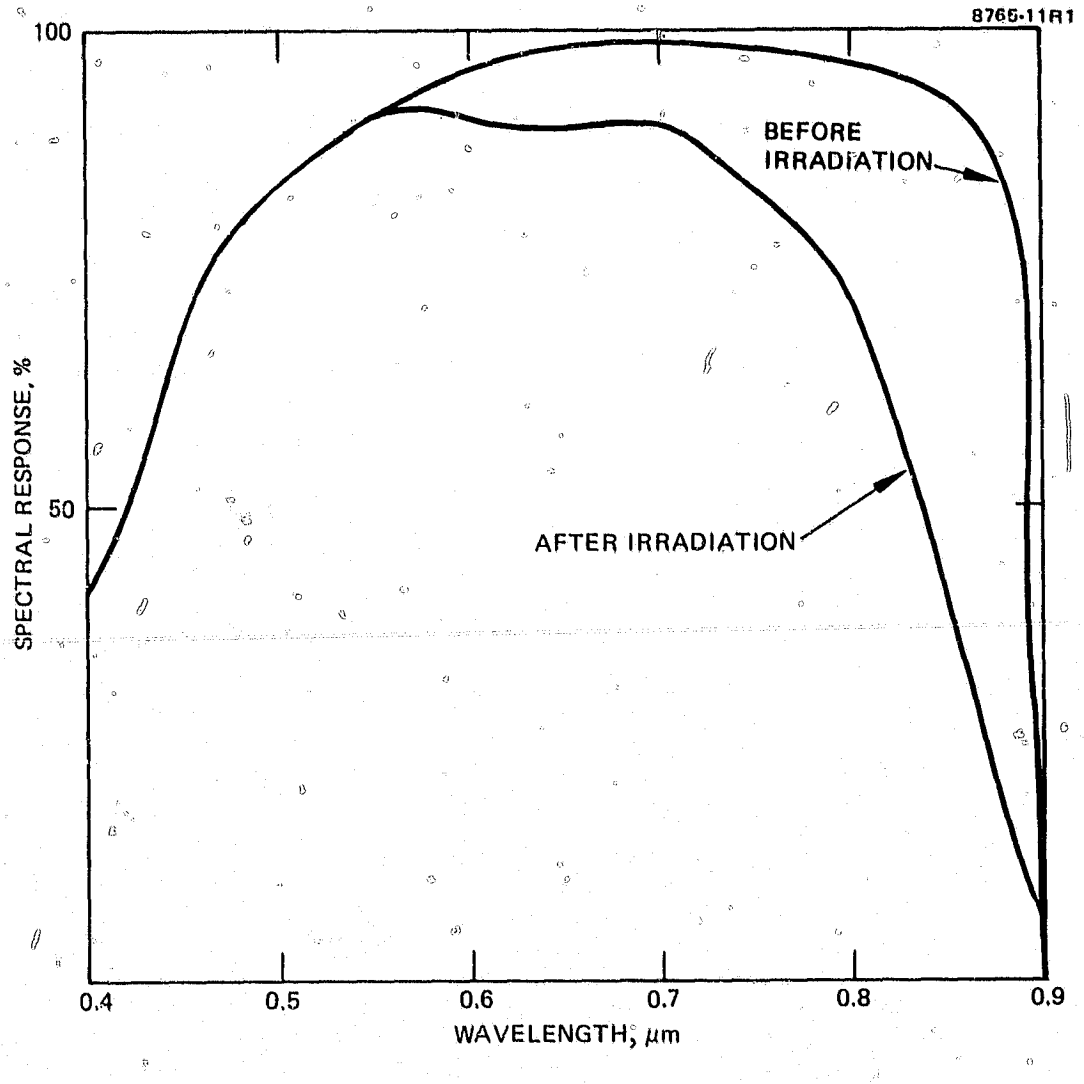

Figure 9. (AlGa)As-GaAs solar cell spectral response (cell 2403, junction depth x_j = 0.5 μm) before and after 1-MeV electron irradiation (fluence = 1 x 10^{15} e cm^{-2}).

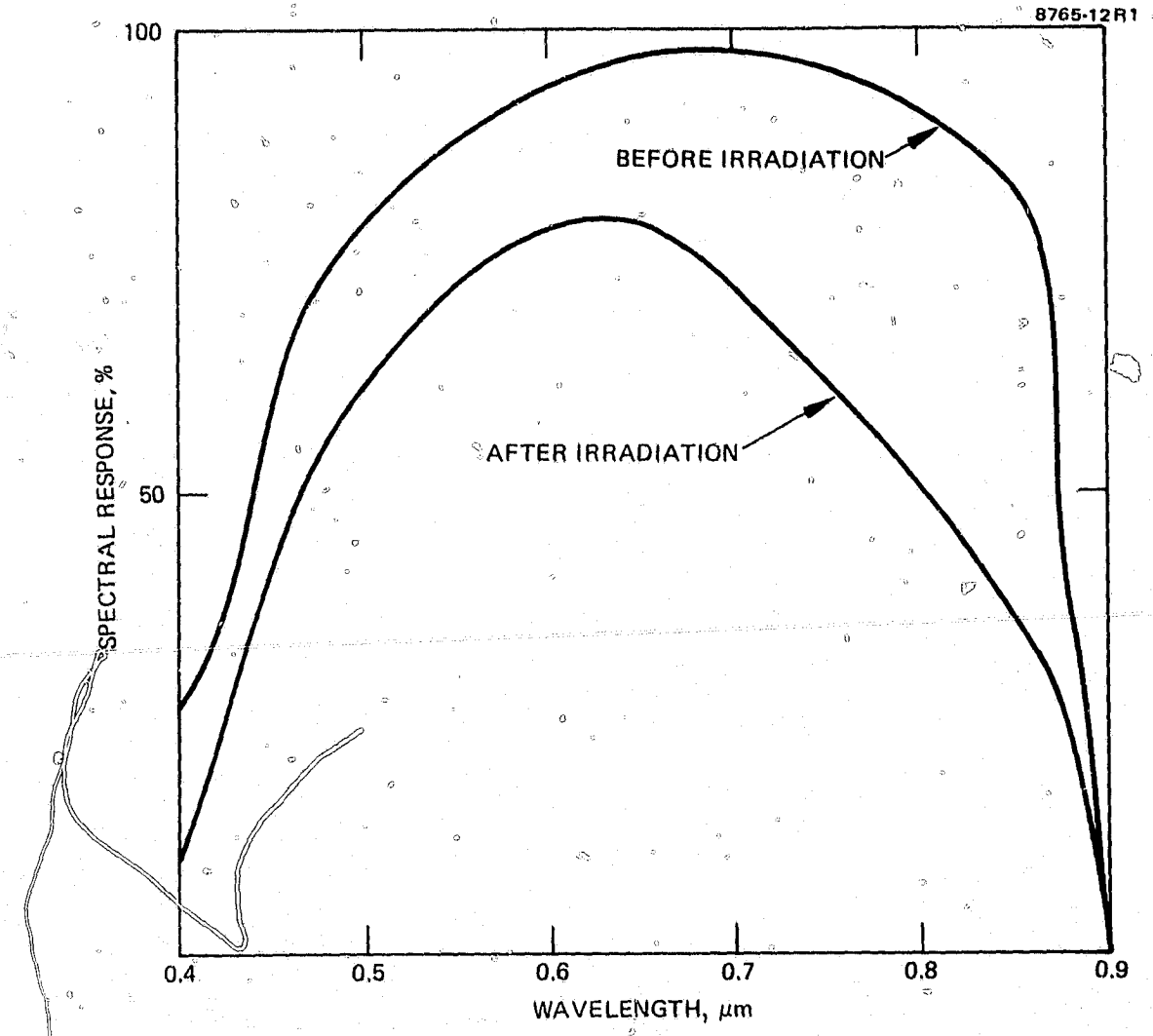

Figure 10. (AlGa)As-GaAs solar cell spectral response (cell 2747, junction depth x_j = 0.5 μm) before and after 1-MeV electron irradiation (fluence = 1 x 10^{16} e cm^{-2}).

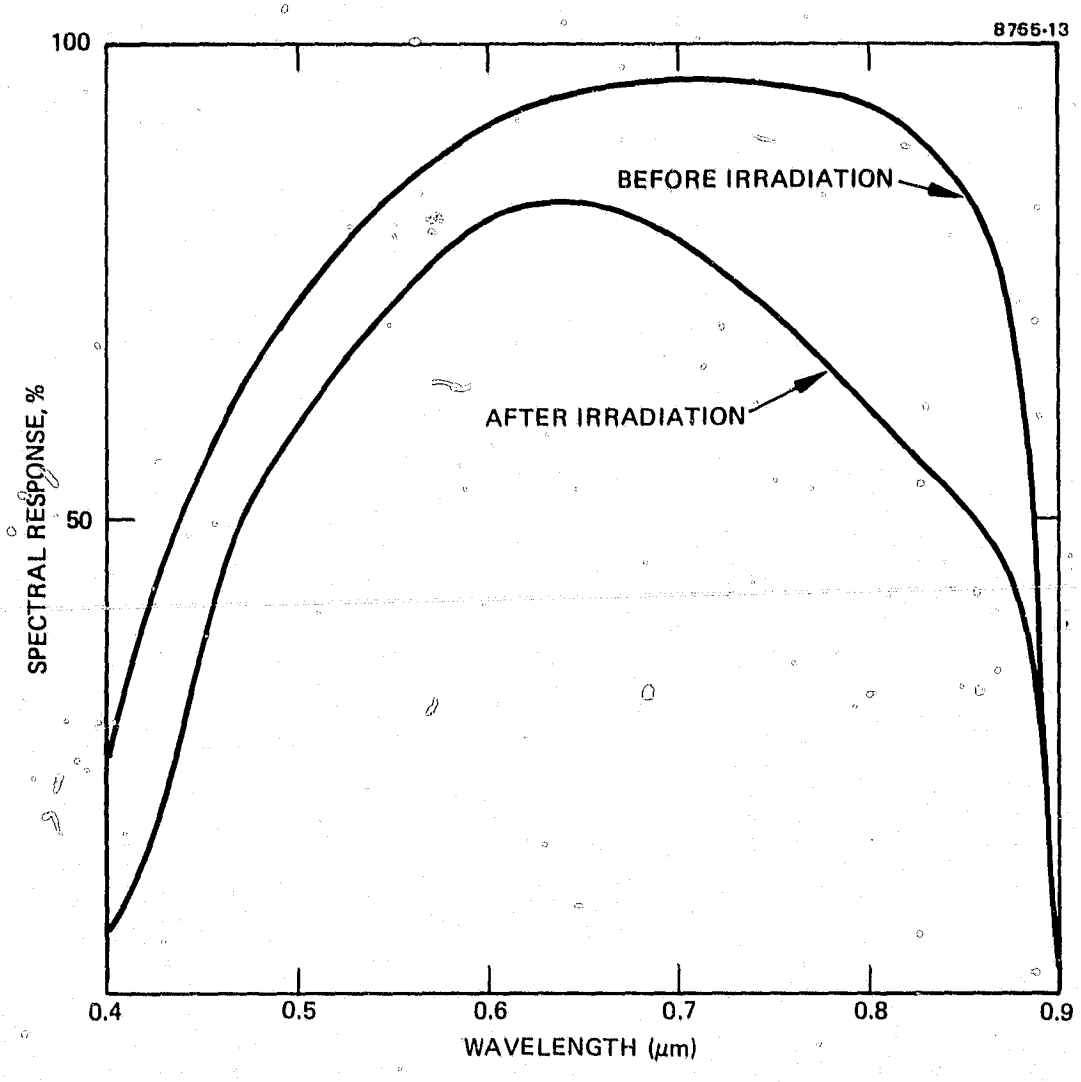

Figure 11. (AlGa)As-GaAs solar cell spectral response (cell 2796, junction depth x_j = 0.3 μm) before and after 1-MeV electron irradiation (fluence = 1 x 10^{16} e cm^{-2}).

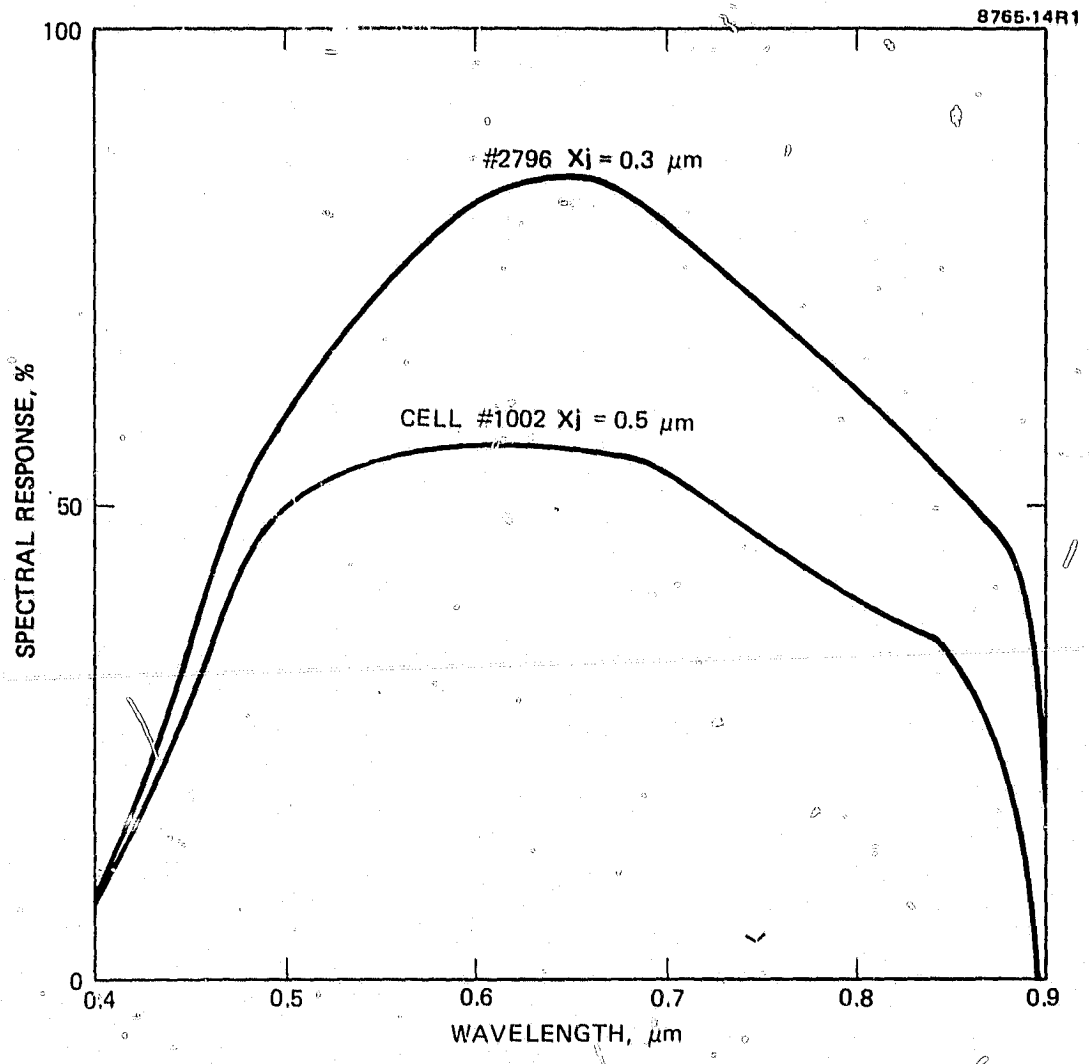

Figure 12. Spectral response after 1-MeV electron irradiation (1×10^{16} e cm^{-2}) for x_j = 0.3 μm and x_j = 0.5 μm (AlGa)As-GaAs solar cells.

As a result of these considerations, it is logical to correlate the improvement in radiation resistance and the improvement in short-wavelength spectral response observed for the same solar cells with decreasing junction depth when these cells are subjected to 1-MeV electron bombardment.

SECTION 4

RADIATION ANNEALING EXPERIMENTS

The thermal annealing experiments on (AlGa)As-GaAs solar cells damaged by 1-MeV electron irradiation were conducted in vacuum at 1×10^{-6} Torr. In this experiment, the solar cells were placed in a small oven that had a resistance heater embedded in the oven wall. A thermocouple was inserted inside the oven beneath the sample and the temperature was controlled within ±5°C. Figure 13 shows a typical temperature cycle for the annealing experiment. Initially the temperature was raised from room temperature to the annealing temperature in 5 to 10 min. Then the temperature was kept stable at this annealing temperature for the total annealing period. The temperature in the oven never exceeded the desired annealing temperature. After the annealing experiment, the solar cells were cooled down to room temperature within 1.5 hr simply by cutting off the supply current to the heater. Two sets of thermal annealing experiments (both isothermal and isochronal) were performed. The first set of experiments consisted of four phase 1 solar cells which were annealed in vacuum (1×10^{-6} Torr) at 200°C for 1 hr, 4 hr, and 9.5 hr. Table 11 gives their individual cell characteristics at each annealing step. Figures 14 through 17 compare the cells' photo I-V and spectral response after thermal annealing with the photo I-V and spectral response before and after electron irradiation. The second set of experiments consists of phase 2 and 3 cells, which were annealed in vacuum (1×10^{-6} Torr) at 200°C, 300°C, 350°C, and 400°C for 0.5 hr at each temperature step. The result is summarized in Figure 3 and Table 12, and Figures 18 and 19 show the photo I-V and spectral response measurements after each anneal step as compared with the measurements before and after electron irradiation. These preliminary results show that:

- Some recovery of the cell performance can be expected at 200°C. This recovery is accelerated by annealing at temperatures above 200°C and occurs in both I_{sc} and V_{oc}. (90% of the initial power is recovered in 0.5 hr after annealing at 400°C).

- There is a significant improvement in the long-wavelength region of the spectral response, which suggests that the annealing leads to a significant recovery in the minority-carrier diffusion length in the bulk of the GaAs after radiation damage.

- The GaAs cells are not damaged either by repeated temperature cycling or holding the cell at 400°C for 0.5 hr.

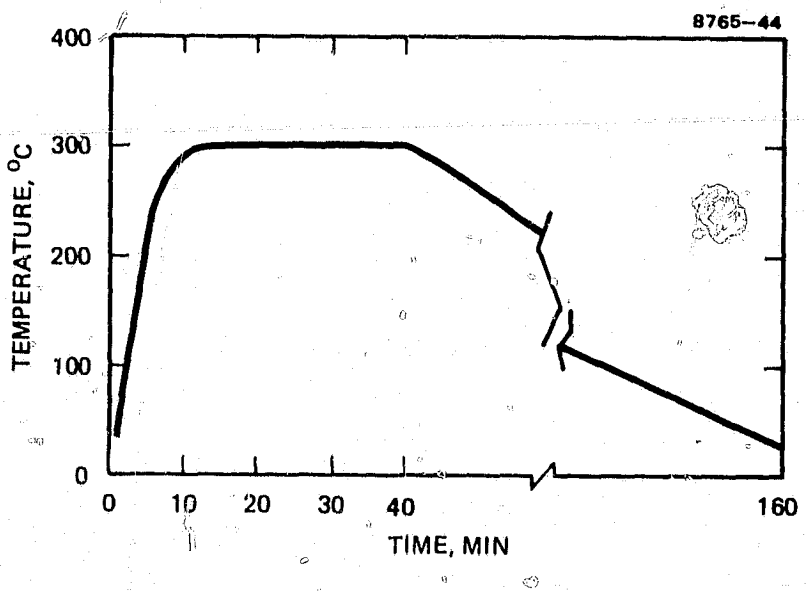

Figure 13.
Typical temperature cycle for the thermal annealing experiment.

Table 11. Thermal Annealing Characteristics of 1-MeV Electron Radiation Damaged (AlGa)As-GaAs Solar Cells

Cell Number	Annealing Temperature, °C	Time, hr	I_{sc}, mA	V_{oc}, V	FF	P_o, mW	η, %	$\frac{P_A}{P_o}$, %
2373	0	0	112	1.0	0.774	86.7	16.0	100.0
			88.5[a]	0.90	0.773	61.6	11.4	71.0
	200	1	92	0.91	0.782	65.5	12.1	75.6
		4	99	0.92	0.778	70.8	13.1	82.0
		9.5	102	0.925	0.775	73.2	13.5	84.4
2401	0	0	111.5	0.99	0.789	87.1	16.1	100.0
			89[a]	0.91	0.80	64.8	12.0	74.5
	200	1	92	0.915	0.808	68	12.6	78.3
		4	100	0.93	0.801	74.5	13.8	85.7
		9.5	105	0.94	0.786	77.6	14.34	89.0
2403	0	0	111	1.0	0.774	85.9	15.9	100.0
			88.5[a]	0.90	0.80	63.91	11.8	74.2
	200	1	93	0.91	0.798	67.55	12.5	78.6
		4	100	0.925	0.799	73.9	13.7	86.2
		9.5	102	0.93	0.787	74.66	13.8	86.8
2405	0	0	110	1.01	0.773	85.9	15.9	100.0
			88.5[a]	0.90	0.80	64	11.82	74.3
	200	1	89.5	0.915	0.797	65.3	12.1	76.1
		4	97	0.93	0.791	71.4	13.2	83.0
		9.5	102	0.935	0.788	75.2	13.9	87.4

[a]After 1-MeV electron irradiation at 1×10^{15} e cm^{-2}.

P_A/P_o = power ratio, where P_A = maximum power after thermal annealing, and P_o = maximum power before electron irradiation.

6664

Table 12. Thermal Annealing Characteristics of 1 MeV Electron Radiation Damaged (AlGa)As-GaAs Solar Cells

Cell Number	Energy	Fluence, e cm^{-2}	Annealing Temperature, °C	Time, hr	I_{sc}, mA	V_{oc}, V	FF	P_{mo}, mW	η, %	$\frac{P_A}{P_o}$, %
2796	0	0	—	—	103.5	0.97	0.81	81.2	15.0	(HRL)
	0	0			103.4	0.957	0.81	80.3	14.8	(JPL)
	1 MeV	1 x 10^{16}	—	—	78	0.815	0.76	48.3	8.9	59.5 (HRL)
			—	—	80.4	0.796	0.77	49.3	9.1	(JPL)
			200	0.5	75	0.825	0.776	48	8.9	59.5 (HRL)
			300	0.5	93	0.91	0.779	66	12.2	81.3 (HRL)
			350	0.5	95	0.93	0.788	69.6	12.9	85.2 (HRL)
			400	0.5	98	0.95	0.784	73.0	13.5	90 (HRL)
2747	0	0	—	—	105	0.98	0.77	79.3	14.6	(HRL)
			—	—	105.4	0.973	0.76	78	14.4	(JPL)
	1 MeV	1 x 10^{16}	—	—	74	0.835	0.759	46.92	8.7	59.2 (HRL)
			—	—	77.5	0.8197	0.767	48.7	9.0	(JPL)
			200	0.5	73	0.84	0.765	46.9	8.7	59.2 (HRL)
			300	0.5	96	0.92	0.764	67.5	12.5	85 (HRL)
			350	0.5	98	0.94	0.759	69.9	12.9	88 (HRL)
			400	0.5	101	0.95	0.74	71.0	13.1	89.5 (HRL)

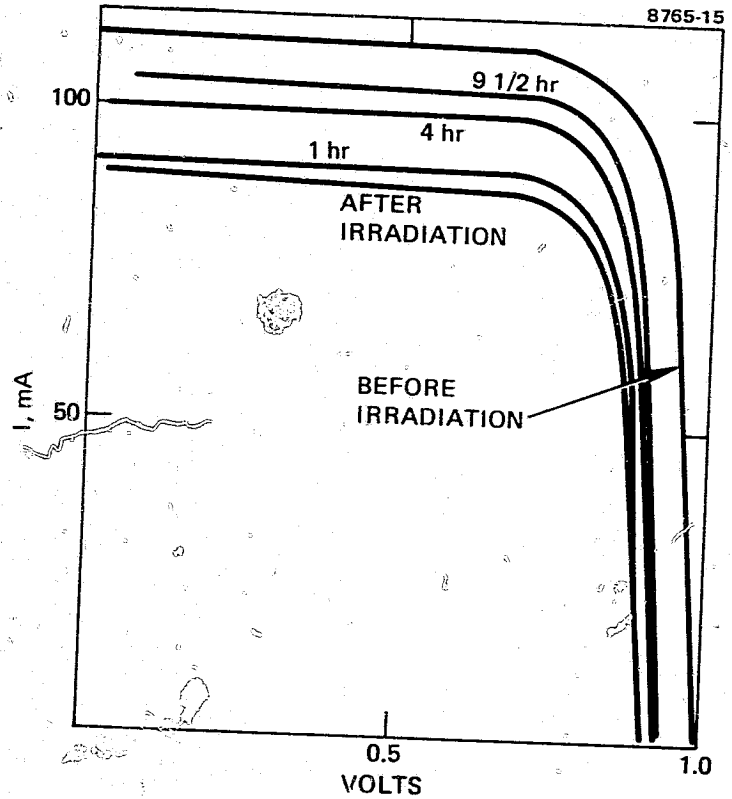

Figure 14(a).
Photo I-V characteristics (cell 2401).

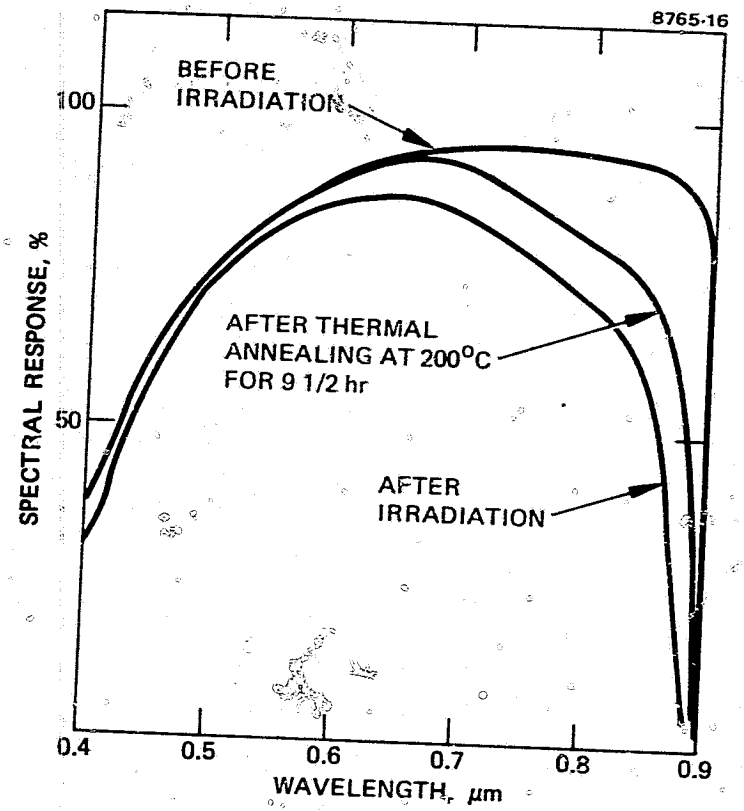

Figure 14(b).
(AlGa)As-GaAs solar cell spectral response
(cell 2401).

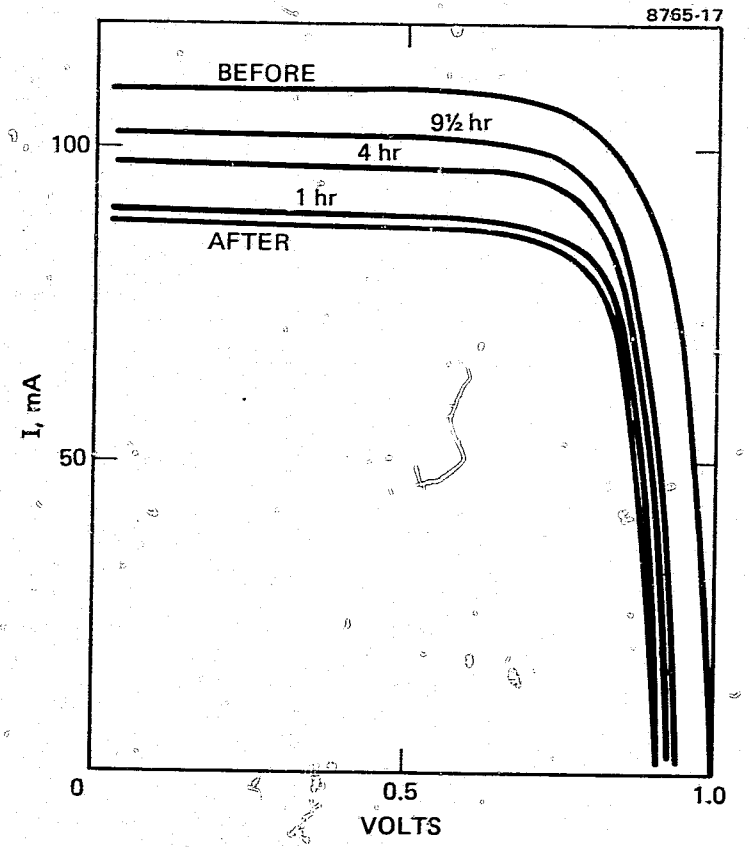

Figure 15(a).
Photo I-V characteristics (cell 2405).

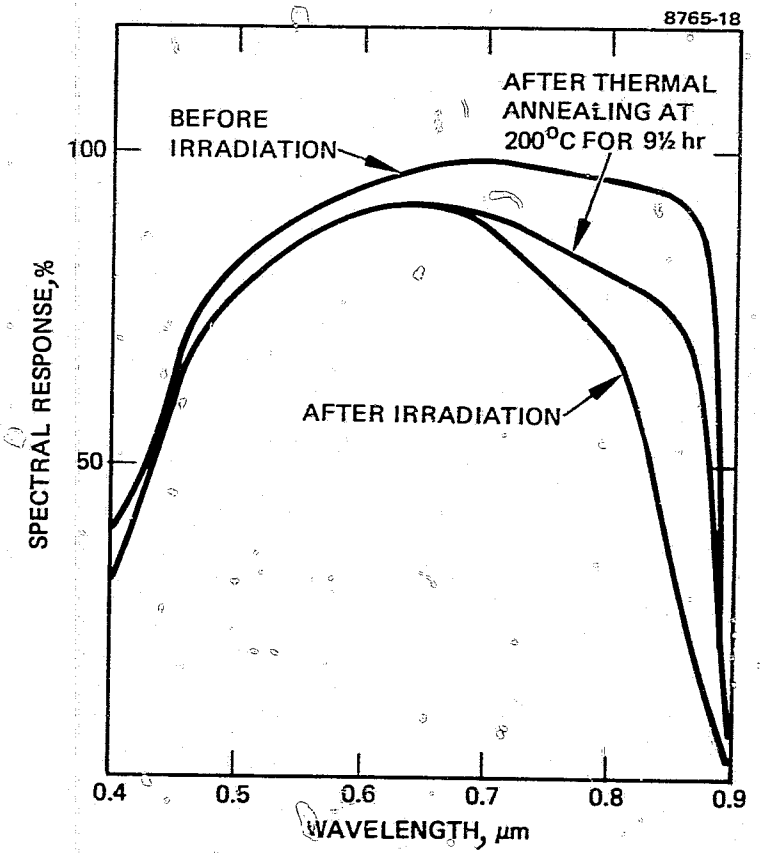

Figure 15(b).
(AlGa)As-GaAs solar cell spectral response (cell 2405).

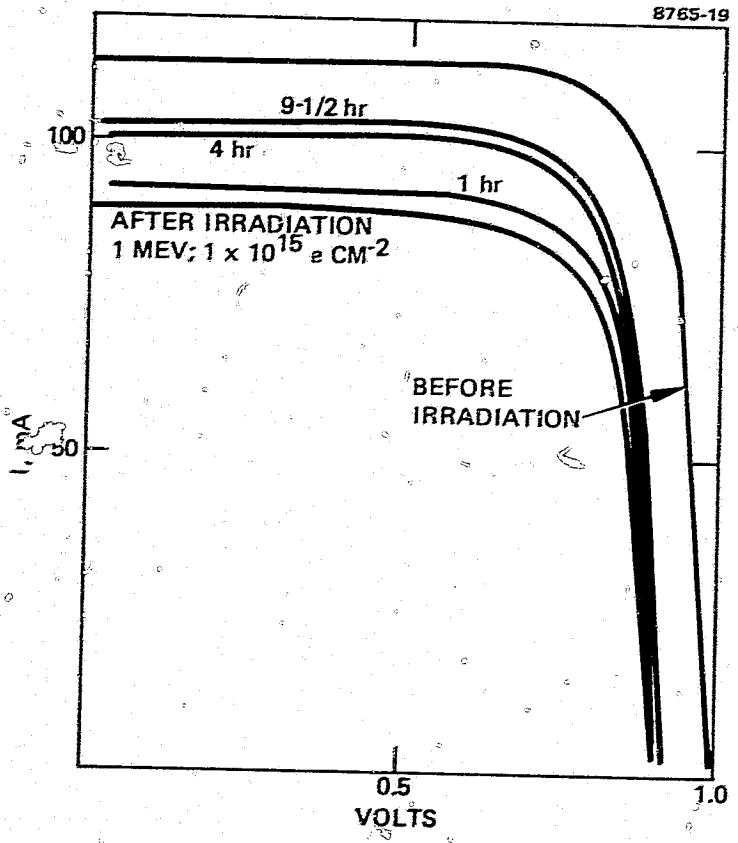

Figure 16(a).
Photo I-V characteristics (cell 2373).
Radiation annealing temperature = 200°C.

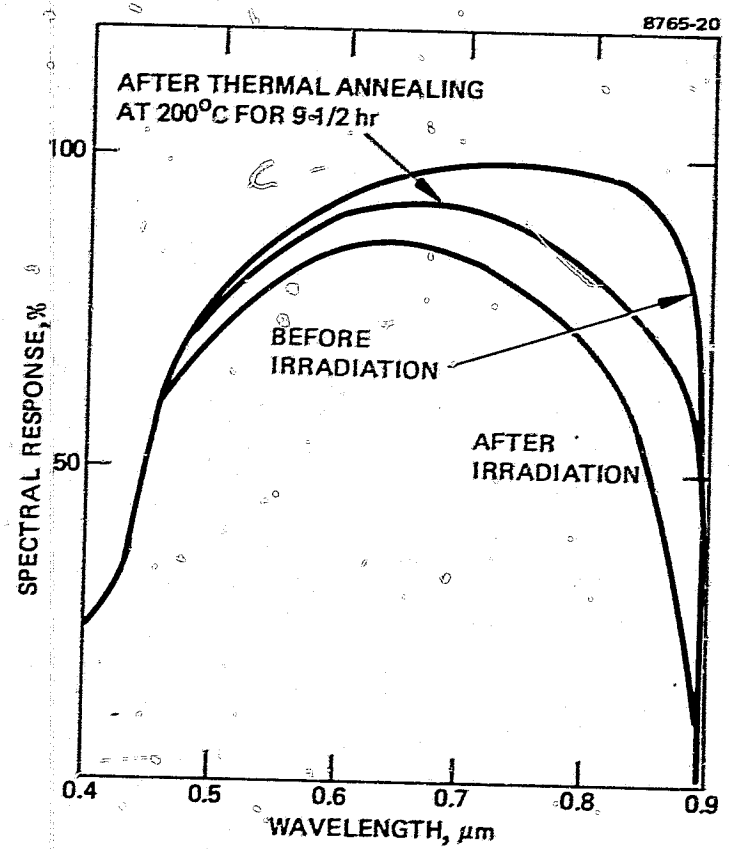

Figure 16(b).
(AlGa)As-GaAs solar cell spectral response
(cell 2373).

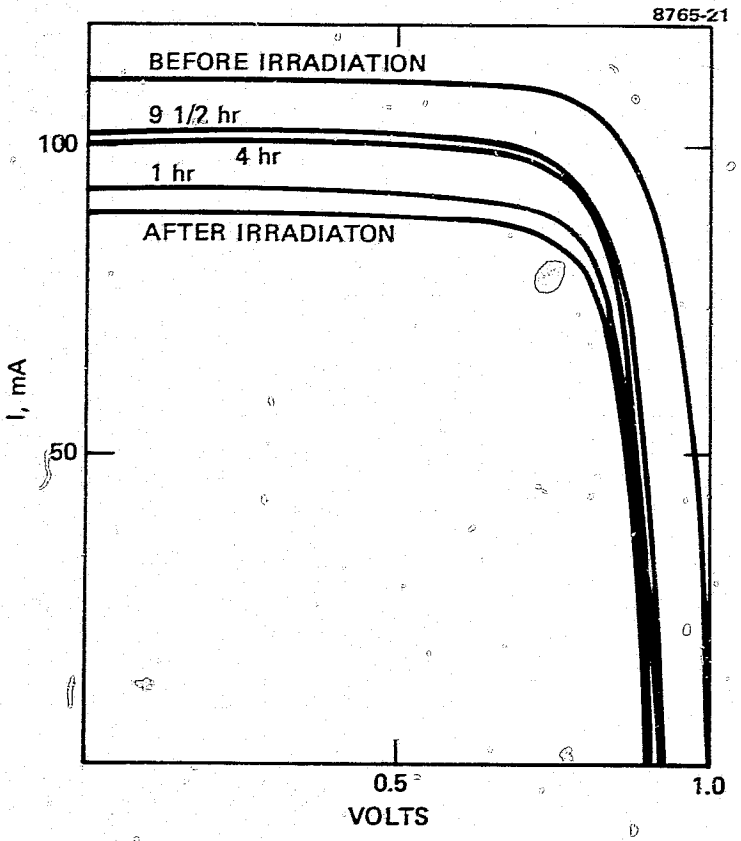

Figure 17(a).
Photo I-V characteristics (cell 2403).

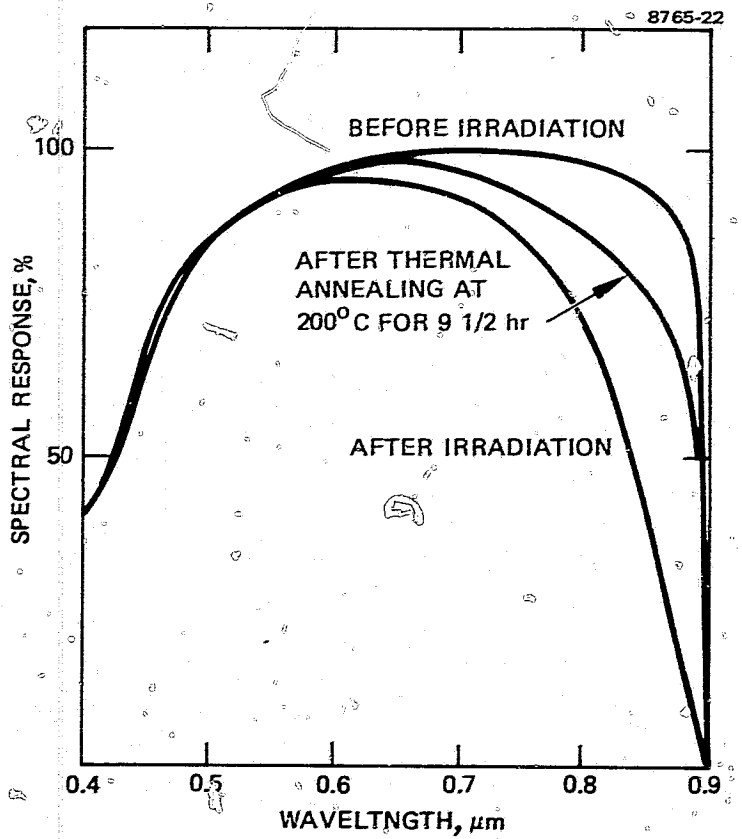

Figure 17(b).
(AlGa)As-GaAs solar cell spectral response
(cell 2403).

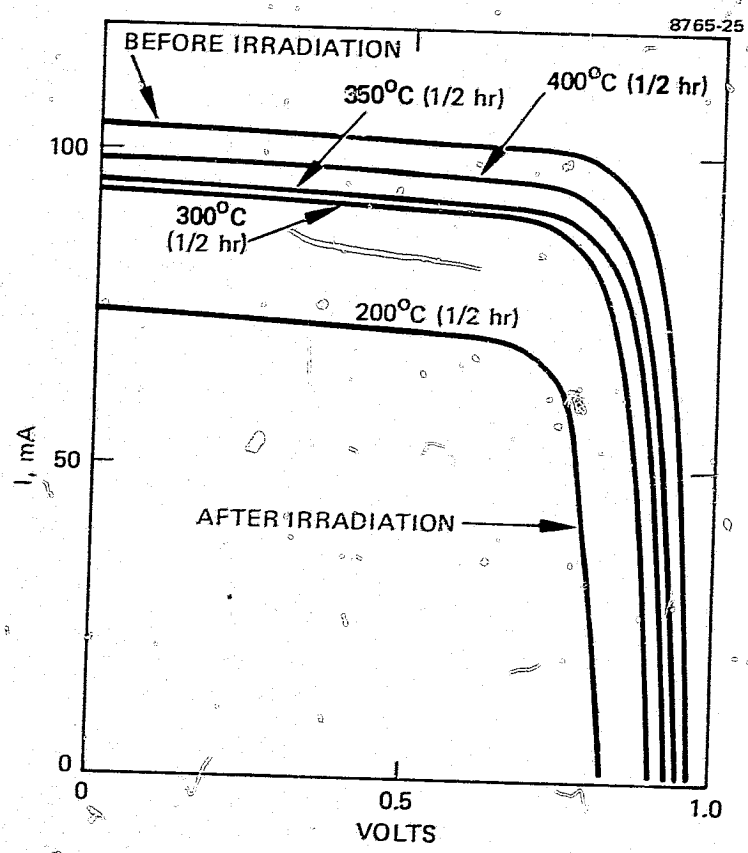

Figure 18(a).
Photo I-V characteristics (cell 2747).

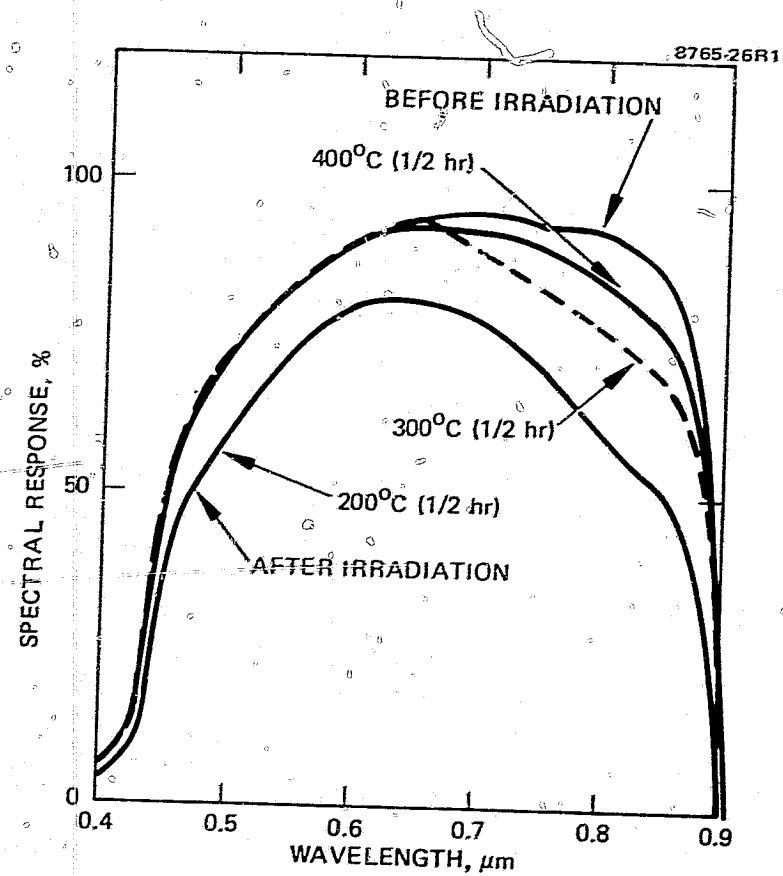

Figure 18(b).
(AlGa)As-GaAs solar cell spectral response (cell 2403).

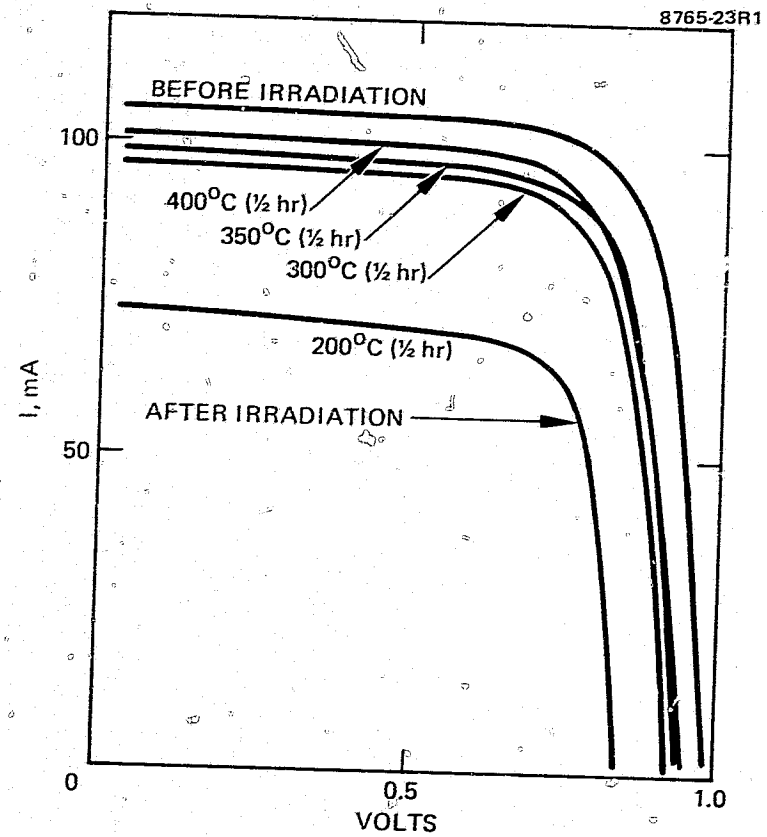

Figure 19(a).
Photo I-V characteristics (cell 2796).

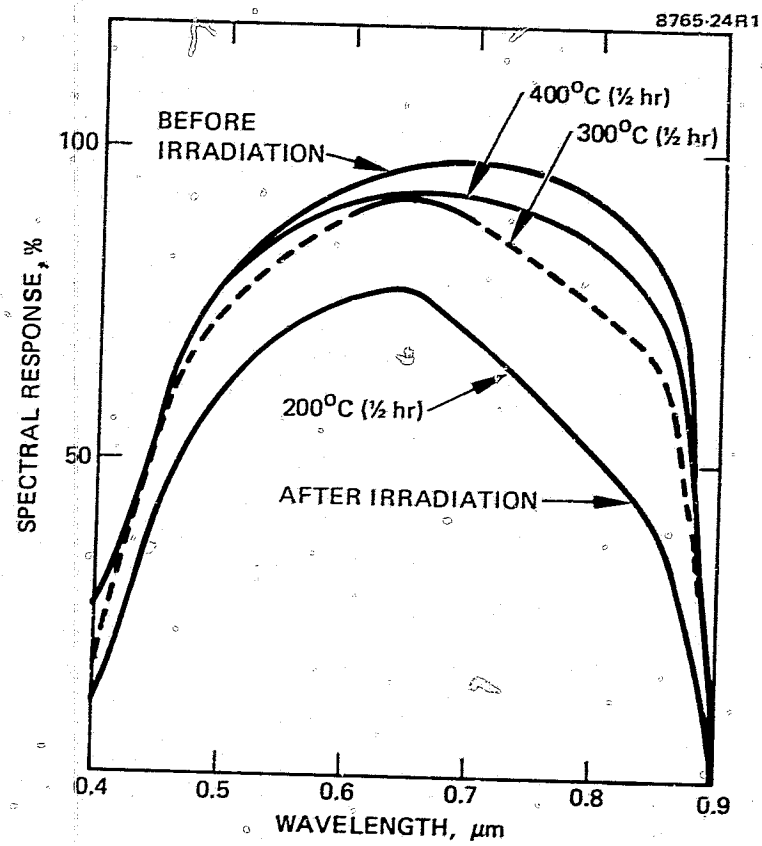

Figure 19(b).
(AlGa)As-GaAs solar cells spectral response (cell 2796).

SECTION 5

CONCLUSION AND SUMMARY

This study confirmed our radiation damage model and has given us a more detailed understanding of the nature of the damage caused by 1-MeV radiation to (AlGa)As-GaAs solar cells. As predicted by our model, the junction depth is a prime factor controlling the extent of damage. The optimum junction depth was found to be relatively shallow ($\sim$0.3 μm). The main factor that leads to this result is the large optical absorption constant in GaAs for the visible solar spectrum. The active region of the cell is only a few micrometers below the cell surface. Thus, in shallow junction cells, it is easy to see that the minority-carrier generated in the p region can reach the junction easily as long as the electron diffusion length is not reduced by the damage to less than the p layer thickness. Under these conditions, the damage is reflected mostly in the long-wavelength region.

We also showed that the cells with 0.3-μm-deep junctions were damaged less than the older cells with 0.5-μm-deep junctions had been. Further improvements in cell performance can be anticipated by lowering the junction depth to about 0.2 μm and also by decreasing the thickness of the (AlGa)As window layer. Both these desirable objectives, however, need careful study since the electrical junction will be located closer to the heterophase boundary and to the surface; the control of the layer perfection and the minimization of interface strain become increasingly important as the junction becomes shallower.

Lowering the doping density in the n region to 1×10^{16} cm^{-3} does not improve the radiation resistance of the cell. Rather, it decreases the open-circuit voltage.

Maintaining the cells at 126°C during irradiation and lowering the irradiation flux rate to 2×10^{10} e cm^{-2} s^{-1} do not reduce the radiation damage. The 126°C temperature seems to be too low to show any annealing effect (at least not over only a few hours) on electron-damaged GaAs solar cells. However, the radiation-damaged solar cells do recover their efficiency when annealed in vacuum (1×10^{-6} Torr) at temperatures as low as 200°C. At temperatures above 200°C, the recovery is accelerated, and at least 90% of the initial power can be recovered. All these GaAs solar cells were subjected to many thermal cycles and kept at 400°C for 30 min. The cells did not show any sign of degradation under these conditions.

The present study indicates the direction for further improvements in the performance of the GaAs cells in radiation environments. A principal area is a further reduction of the junction depth; however, this must be achieved without affecting the quality of the electrical junction by proximity to the heterophase boundary and to the cell surface. Both these are stringent requirements and need careful tailoring of the cell structure, especially since the cell area is relatively large. The second area requiring investigation is the annealing behavior of radiation-damaged cells. The effect of thermal annealing on the various components of the cell structure can be resolved by detailed studies of the electrical and optical characteristics of the cells before and after radiation. Such studies are essential to achieving a systematic understanding of the cause and minimization of the damage caused by both electrons and particles such as protons and neutrons. A detailed understanding of these factors can enhance the GaAs cell performance for the near-sun solar missions contemplated by JPL.

APPENDIX A

This paper was presented to the 13th Photovoltaic Specialists Conference, June 1978 at Washington, DC.

ELECTRON AND PROTON DEGRADATION IN (AlGa)As-GaAs SOLAR CELLS

R. Loo, L. Goldhammer,* B. Anspaugh,** R.C. Knechtli and G.S. Kamath

Hughes Research Laboratories
Malibu, California 90265

ABSTRACT

Results on radiation damage in (AlGa)As-GaAs solar cells by 1 MeV electron fluences up to 1×10^{16} e/cm^{-2} and by 15, 20, 30 and 40 MeV proton fluences up to 5×10^{11} P cm^{-2} are presented. The damage is compared with data on state-of-the-art silicon cells which were irradiated along with the gallium arsenide cells. We verified experimentally our theoretical expectation that the junction depth has to be kept relatively shallow, to minimize radiation damage. The damage to the GaAs cells as a function of irradiation, is correlated with the change in their spectral response and dark I-V characteristics. The effect of thermal annealing on the (AlGa)As-GaAs solar cells was also investigated. This data is used to predict further avenues of optimization of the GaAs cells.

INTRODUCTION

The behavior of solar cells under radiation environment is of great importance for space application. Previous studies have shown that the (AlGa)As-GaAs solar cells have achieved an efficiency of 18.5% AMO (1) with a radiation resistance equal to or better than that observed in violet silicon cells (2). In this paper, we report the radiation effect on large-area (2 cm x 2 cm) (AlGa)As-GaAs solar cells fabricated at Hughes Research Laboratories (HRL) using the infinite melt liquid phase epitaxial (LPE) growth system. Our best cell to date has an AMO efficiency of 18%, and our improved shallow-junction cells show more radiation resistance than silicon cells.

GaAs has a large optical absorption constant and a short diffusion length; essentially, all the photovoltaic response is close to the GaAs surface. The radiation damage beyond this active region has a negligible effect on cell performance. Consequently, the reduction in the required minority carrier diffusion length and the relative shallowness of the active region are the key factors that can be exploited to make GaAs solar cells more radiation resistant. Data consistent with these observations is presented below.

*Hughes Aircraft Company, El Segundo, California
**J.P.L., Pasadena, California

EXPERIMENTAL

Figure 1 shows the (AlGa)As-GaAs solar cell structure. The n^+ concentration for the substrate is fixed at > 5×10^{17} cm^{-3} with Te as the dopant. The n buffer layer concentration is 1×10^{17} cm^{-3}. (At this doping level, the open-circuit voltage is 1 V.) The thickness of this layer was fixed at 10 μm or more because results indicated that the substrate visibility is minimized at a buffer layer thickness of 10 μm. A thickness less than this is not always sufficient to remove the effect of the substrate on cell performance.

7545-6

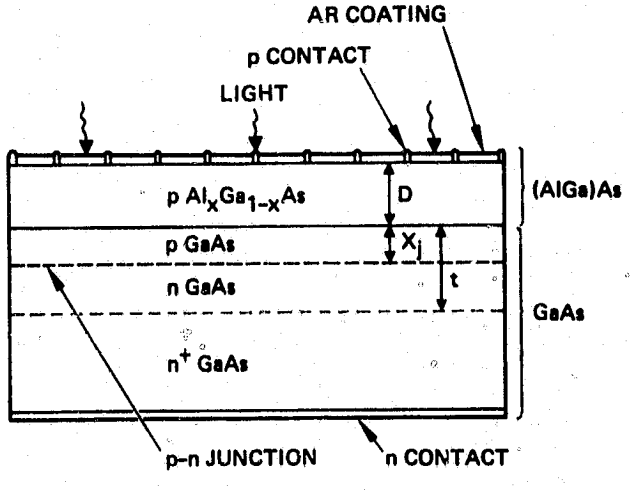

NUMBER OF FINGERS = 24
p CONTACT: Au-Zn-Ag
n CONTACT: Au-Ge-Ni-Ag
AR COATING: Ta_2O_5
p $Al_xGa_{1-x}As$: $X \geq 0.95$
CELL SIZE = 2 x 2 CM^2

Figure 1. The (AlGa)As-GaAs solar cell

The window layer of $(Al_xGa_{1-x})As$ is grown by LPE on GaAs. Our layer has $x > 0.90$, making the bandgap and hence the optical transmission as high as possible. The dopant is beryllium (Be). The concentration is 1×10^{18} cm^{-3}. During (AlGa)As window layer growth, a p-n homojunction is formed by Be diffusion from the (AlGa)As layer into the n buffer layer. The carrier concentration of the p-diffused region is also 1×10^{18} cm^{-3}.

The remaining parts of the baseline structure are self-explanatory. The Au-Zn contacts are about 3000 to 4000 Å with a silver overlay about 4 µm thick, and the n contact is AuGeNi (∿ 5000 Å) with an Ag overlay. The AR coating is Ta_2O_5.

The Dynamitron particle accelerator at JPL was used as the electron source for high-energy electron irradiation; the irradiations were performed in vacuum at room temperature. The uniformity over the test plane was ± 4% with no areas of discontinuity. Fluxes and fluences were measured with a Faraday cup the current of which was integrated to establish electron fluences and to automatically stop the irradiation at the desired fluence levels.

High-energy proton irradiation was performed at the Crocker Nuclear Laboratory at the University of California at Davis. This cyclotron can produce a primary proton beam at energies between approximately 8 and 68 MeV. The solar cells were mounted with small pieces of double-face masking tape to aluminum plates. Each plate was irradiated separately in air at specific proton energies and fluences.* The fluence over the target plane was uniform within ±5%. The cell temperature during irradiation was kept at 30°C.

The full matrix of tests performed on the (AlGa)As-GaAs solar cells and on several representative silicon solar cells are given in Tables 1 and 2.

Table 1. Electron Irradiation Experiments

7545-4

ELECTRON ENERGY MeV	ELECTRON FLUENCE E/CM^2	TYPE AND NUMBER OF CELLS		
		(AlGa)As-GaAs	Si CONVENTIONAL	Si HIGH EFFICIENCY
1.0	1×10^{13}	3	3	3
	4×10^{14}	3	3	3
	1×10^{15}	3	3	3
	5×10^{15}	3	3	3
	1×10^{16}	3	3	3
0.7	1×10^{15}	2		
1.9	1×10^{15}	2		

Table 2. High-Energy Proton Irradiation Experiments

7545-5

PROTON ENERGY MeV	PROTON FLUENCE E/CM^2	TYPE AND NUMBER OF CELLS		
		(AlGa)As-GaAs	Si HIGH EFFICIENCY	Si CONVENTIONAL
15.4	5×10^{10}	3	5	4
15.4	5×10^{11}	3	4	4
22	5×10^{10}	3	2	3
22	5×10^{11}	3	2	3
30	5×10^{10}	3	2	3
30	5×10^{11}	3	2	3
40	5×10^{10}	3	2	3
40	5×10^{11}	3	2	3

RESULTS AND DISCUSSION

Electron Damage

A group of cells were fabricated early in the program for electron radiation tests. These cells were designed to have high efficiency with no attempt at optimizing the design parameters to increase radiation hardness. Figure 2 shows the maximum power obtained from the cells plotted against 1 MeV electron radiation fluence. These results were then compared with those for two types of silicon cells as shown in Table 1. This showed the need to improve these early cells for better resistance to electron radiation damage at fluences in excess of 4×10^{14}/cm^2.

Figure 3 shows the spectral response before and after electron irradiation. The results show that in these cells the spectral response in the short wavelength region shows greater damage compared to the longwavelength region. Since the optical absorption coefficient is greater for short wave lengths, most of the absorption in this region will be close to the surface of the cell. The photo generated carriers, therefore, must travel farther to reach the junction than do those generated by longer wavelengths. We suspected from the spectral response of the damaged cells that their junctions had to be relativily deep compared to the minority carrier diffusion length in the damaged layer. Our suspicion was confirmed by the measured junction depth of ≥ 1 µm. These observation led us to examine the influence of the junction depth on radiation damage more carefully.

*By comparing the results from previous solar cells irradiated both in air and in vacuum, we found that the ionized gases in air surrounding the cell during irradiation have no effect on the cells.

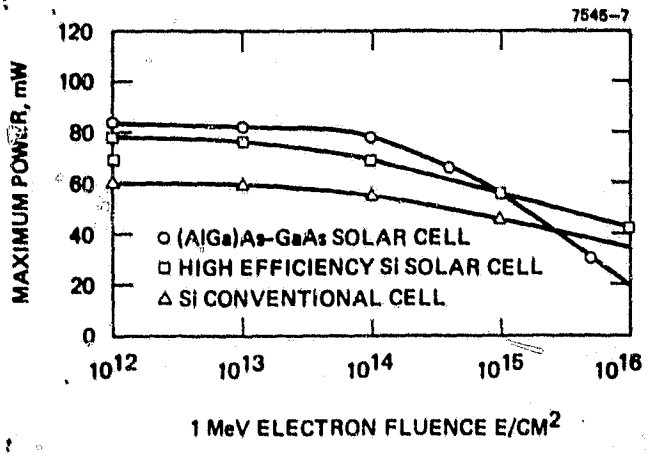

Figure 2. Maximum power as a function of 1 MeV electron fluence

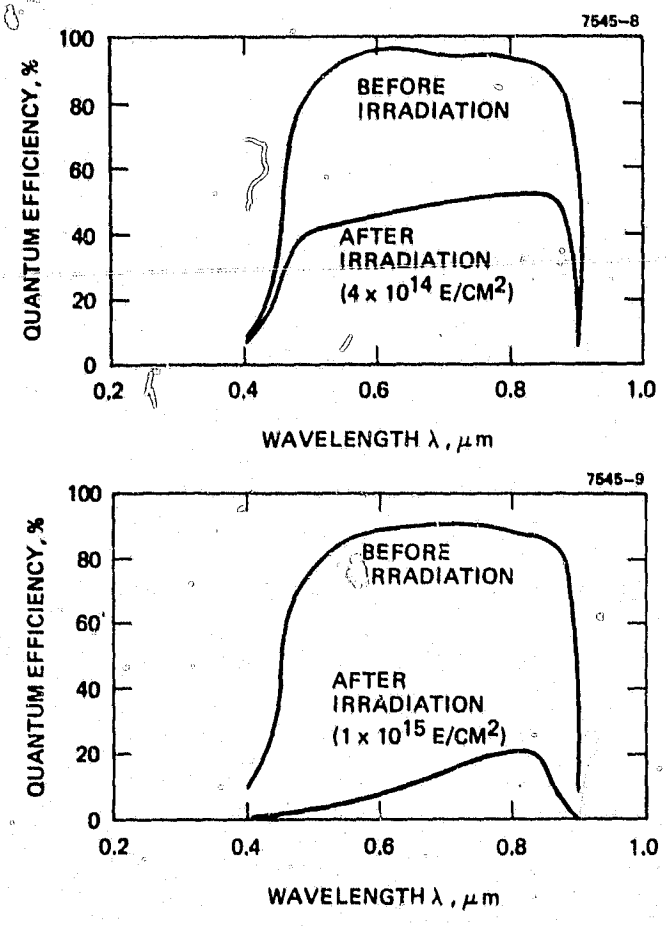

Figure 3. (AlGa)As-GaAs solar cell spectral response before and after 1 MeV electron irradiation

To correlate theory and experiments, Figure 4 shows the (AlGa)As-GaAs solar cell short circuit current density as a function of 1 MeV electron radiation fluence. The continuous curve represents the normalized experimental values. The dotted

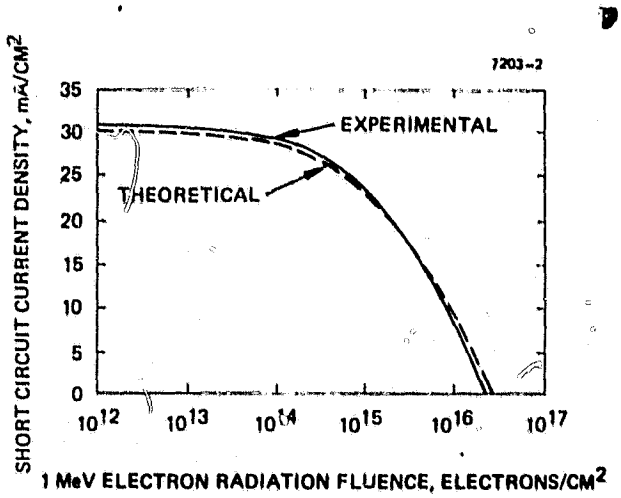

Figure 4. Short circuit current density versus 1 MeV electron radiation fluence, electrons/cm^2

line is the theoretical curve. Both curves correspond to an (AlGa)As layer thickness of 1 μm and a junction depth of 1 μm. For calculating the theoretical curve, the minority carrier diffusion length L was related to the fluence ϕ by the usual relation:

$$\frac{1}{L^2} = \frac{1}{L_o^2} + K_L \phi \quad . \qquad (1)$$

The initial diffusion lengths for holes (L_{po}) and electrons (L_{no}) were assumed to be 2 and 5 μm, respectively in these calculations. The damage constant K_L for the diffusion length used for both p- and n-type GaAs was deduced by matching the theoretical curve to the experimental curve as shown in Figure 4. It was found to be $K_L = 7 \times 10^{-8}$, assuming the same value of K_L for the n- and p-doped GaAs.

Using this value for K_L, the short-circuit density was calculated for several junction depths as a function of a 1 MeV electron fluence. The results, shown in Figure 5, show that radiation damage decreases as junction depth decreases.

Based on this analysis, we proceeded to fabricate a second-generation of (AlGa)As-GaAs solar cells with the goal of decreased sensitivity to the radiation environment. The window layer thickness was made at 0.5 μm while the junction depth was decreased to ∿ 0.5 μm by readjusting the LPE layer growth parameters.

Figure 6 shows the measured short-circuit current of these shallower junction cells versus 1 MeV electron fluence. The experimentally observed improved radiation resistance is in good agreement

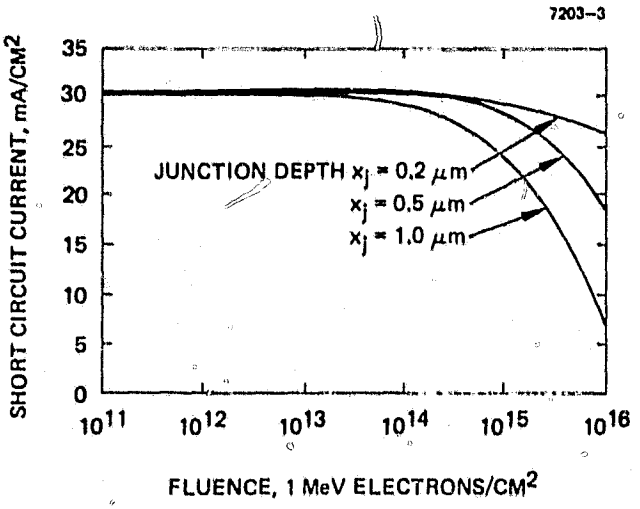

Figure 5. Predicted (AlGa)As-GaAs solar cell short circuit current density versus 1 MeV electron radiation fluence ((AlGa)As layer thickness = 1.0 μm, initial diffusion length L_{po} = 2 μm, L_{no} = 5 μm, and diffusion length damage constant $K_L = 7 \times 10^{-8}$)

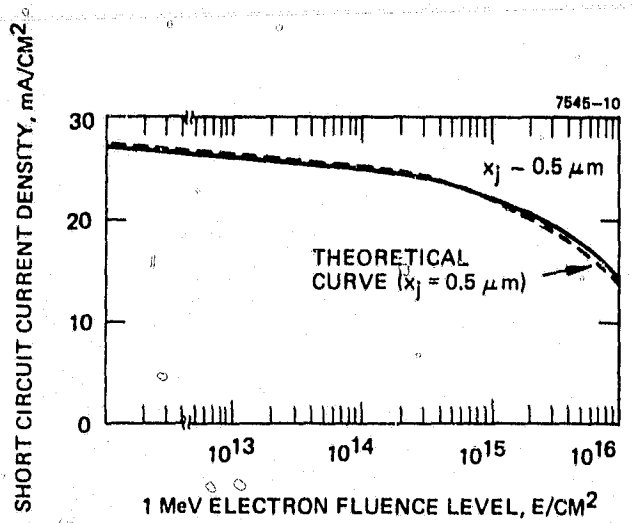

Figure 6. Short circuit current versus electron fluence level (1 MeV)

with the predictions of the theory. Figure 7 shows the experimental results for both (AlGa)As-GaAs solar cells and newly developed high-efficiency Si solar cells as a function of 1 MeV electron irradiation. Also shown for reference are the results of our previous set of irradiated (AlGa)As-GaAs deep-junction solar cells.

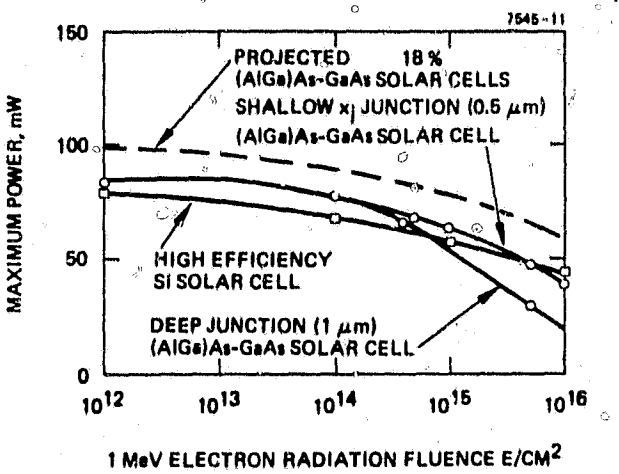

Figure 7. Maximum output power versus 1 MeV electron fluence

The spectral response of the deep-junction and shallower junction cells, both before and after irradiation, are given in Figure 8(a and b). The figure shows that the radiation damage in the deeper junction cells is concentrated in the short-wavelength region, whereas the shallower junction causes the damage to shift to the longer wavelength. This is consistent with our observation that the collection of minority carriers in the p region is not much affected up to the fluence at which the electron diffusion length is reduced to less than the p layer thickness.

Figure 8(c) shows the spectral response of the shallower junction solar cells irradiated at fluences 1×10^{15} e/cm^2 with electron energies varying from 0.7 MeV to 1.9 MeV. As expected at higher energies, these cells show more degradation, probably because K_L increases with increasing electron energy. Figure 9 shows typical dark current-voltage (I-V) characteristics before and after electron irradiation. Although solar cells become more leaky after irradiation, the basic transport mechanism remains the same (as shown by the I-V curves, which remain parallel to each other). This increased leakage current probably results from an increase in the number of recombination centers at the junction.

High Energy Proton Damage

Twenty-four (AlGa)As-GaAs solar cells and several representative silicon cells were irradiated with 15.4 MeV to 40 MeV protons at fluences of 5×10^{10} and 5×10^{11} p/cm^2 (Table 2).

The baseline structure of the solar cell used for proton irradiation was the same as that of the shallow-junction solar cells used for electron

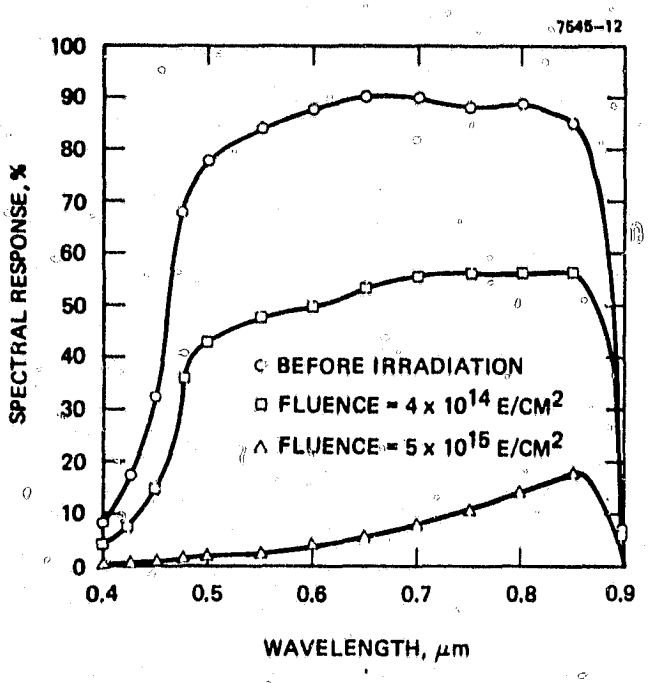

Figure 8(a). (AlGa)As-GaAs solar cell spectral response versus 1 MeV electron radiation fluences

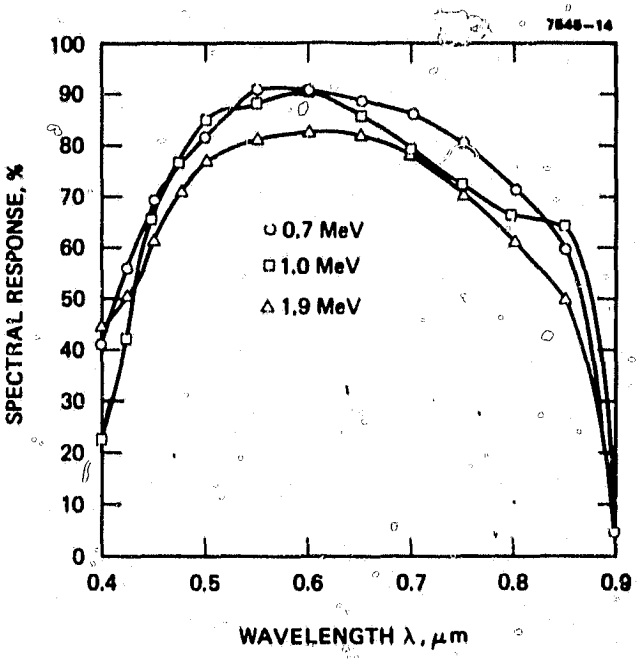

Figure 8(c). (AlGa)As-GaAs solar cell spectral response for several electron energies

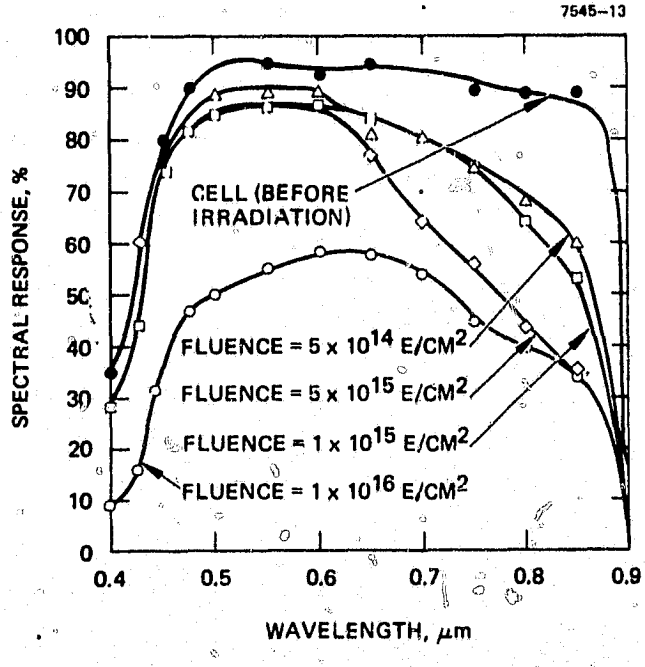

Figure 8(b). (AlGa)As-GaAs solar cell spectral response versus 1 MeV electron radiation fluence

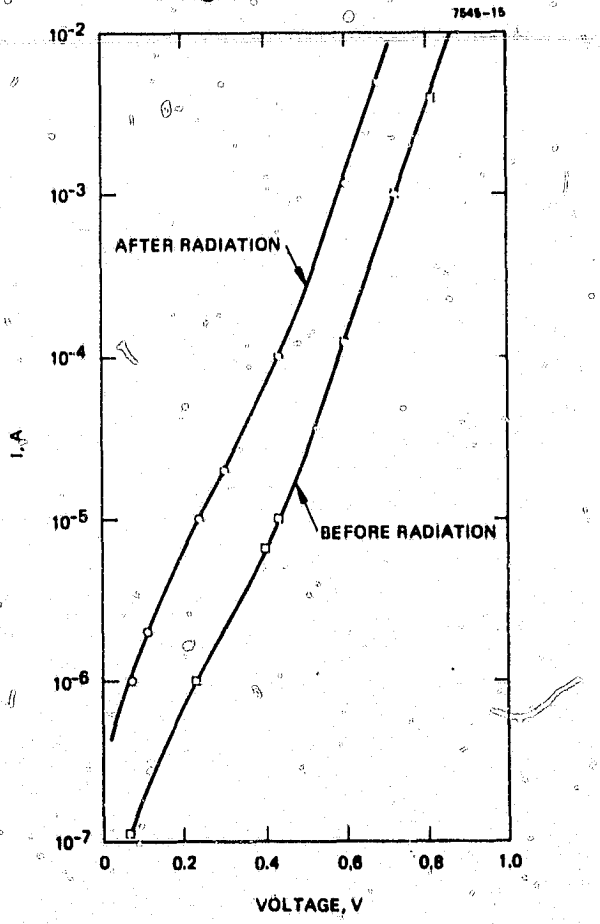

Figure 9. Dark I-V characteristics before and and after electron irradiation

irradiation, except that no cover glass was applied to these cells.

The results of these proton irradiation tests are summarized in Figure 10 (a and b), which shows the maximum solar cell output power versus proton irradiation fluence for the three types of cells specified in Table 2. The (AlGA)As-GaAs solar cells are more resistant to high-energy proton radiation damage than the silicon cells. The dotted lines plotted in Figure 10 are extrapolations of our test results; these show the effect expected from proton fluence on an improved (AlGa)As-GaAs solar cell with a beginning-of-life AMO power-conversion efficiency of 18%. This extrapolation is pertinent since the feasibility of an 18% efficiency has already been demonstrated for this type of cell.

Figures 11 and 12 show the average spectral response of the (AlGa)As-GaAs solar cells before and after proton irradiation with proton energies of 15.4 MeV and 40 MeV, respectively. The spectral response in the short wavelength region of these shallow-junction solar cells is almost insensitive to the proton irradiation. A slight decrease in the solar cell spectral response occurs only in the long wavelength region.

Figure 13 shows the dark I-V characteristic before and after irradiation. Again, just as in the case of electron irradiation, the solar cell junction becomes slightly leaky due to the increasing number of recombination centers produced by proton irradiation although the basic transport mechanism remains unchanged.

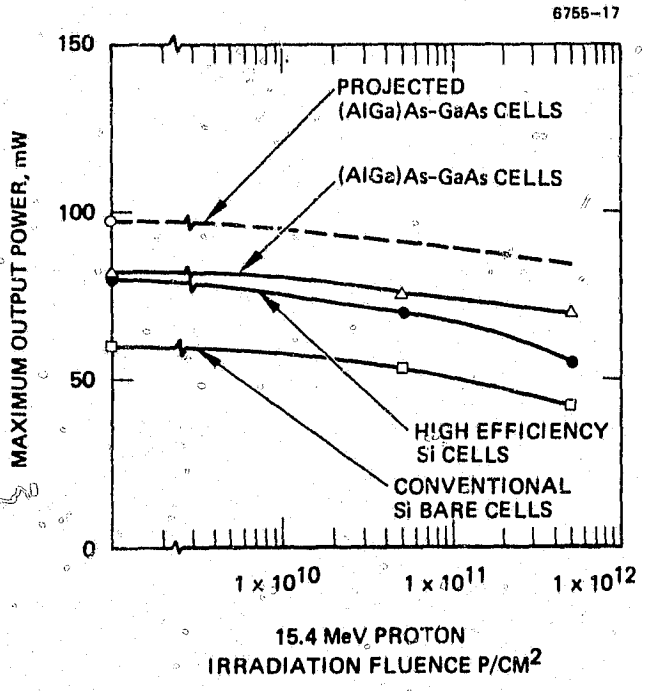

Figure 10(a). Solar cell maximum output power versus 15.4 MeV proton irradiation fluence.

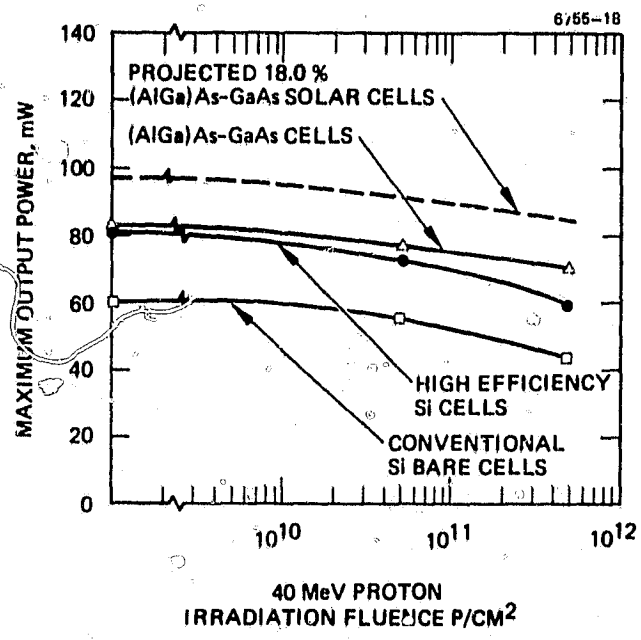

Figure 10(b). Solar cell maximum output power versus 40 MeV proton irradiation fluence

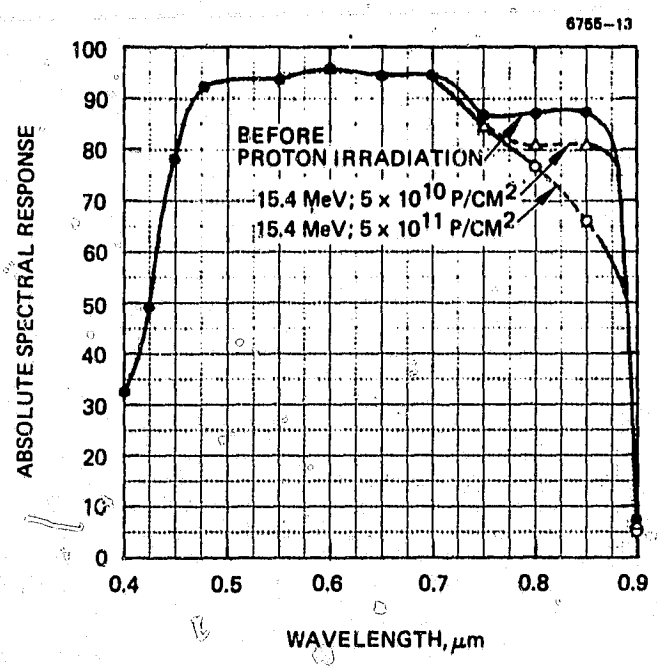

Figure 11. (AlGa)As-GaAs solar cell spectral response before and after 15.4 MeV proton irradiation

Radiation Annealing Studies

GaAs solar cells damaged by radiation recover their efficiency when annealed at low temperatures

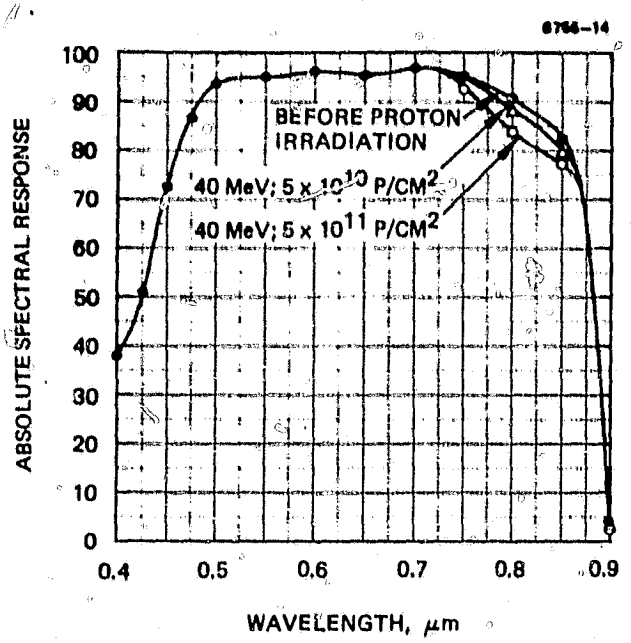

Figure 12. (AlGa)As-GaAs solar cell spectral response before and after 40 MeV proton irradiation

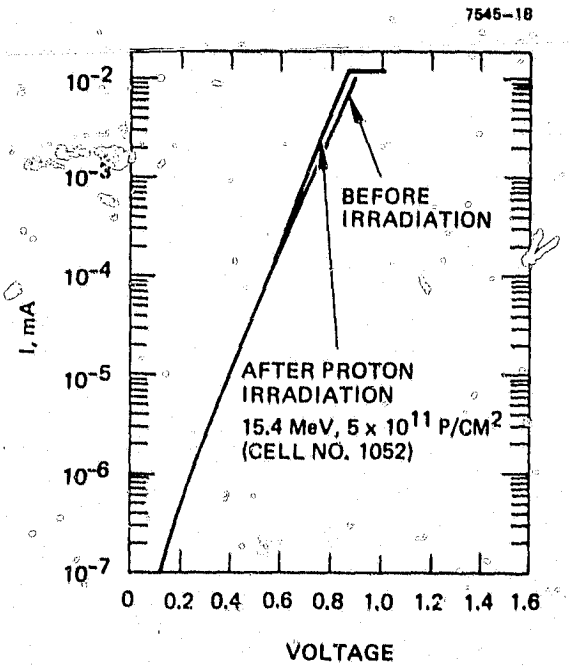

Figure 13. Dark I-V characteristics before and after proton irradiation

Figure 13. Dark I-V characteristics before and after proton irradiation

on the order of 200°C to 300°C (3,4). Some preliminary thermal annealing experiments on the radiation-damaged (AlGa)As-GaAs solar cells were performed in our laboratory. The cells were irradiated at fluences of 1 x 10^{15}/cm^2 with electron energies varying from 0.7 MeV through 1.0 MeV to 1.9 MeV. Subsequently, they were annealed in vacuum at temperatures of over 200°C. Figure 14 shows the effect of annealing as a function of annealing time and temperatures.

Figure 15 compares the spectral response of these cells after the annealing step with the spectral response before and after electron irradiation. The long wavelength region shows significant recovery. This suggests that the annealing leads to a significant recovery in the minority carrier diffusion length in GaAs after radiation damage.

Figure 16 shows the dark I-V characteristics of these cells. These cells show leaky p-n junctions after irradiation; however, they almost completely recover to their pre-irradiation condition after annealing at 210°C. These results indicate that (AlGa)As-GaAs solar cells can be annealed at practical temperatures to remove radiation damage. This could be exploited for longer space missions.

CONCLUSION AND SUMMARY

Several 2 cm x 2 cm (AlGa)As-GaAs cells were subjected to radiation damage studies using both electrons and protons. The results show that:

- (AlGa)As-GaAs solar cells can be made more resistant to radiation damage than can silicon cells for both electron and proton irradiation.
- The junction depth is a sensitive parameter in determining radiation resistance.
- The (AlGa)As-GaAs solar cells suffer only a moderate amount of degradation at proton energies above 15.4 MeV.
- The efficiencies of electron-radiation-damaged (AlGa)As-GaAs solar cells recover when annealed at temperatures as low as 200°C to 300°C.

ACKNOWLEDGMENT

The radiation damage studies reported here were supported in part by contracts from NASA Langley, Contract NAS 1-14727

REFERENCES

1. J.M. Woodall and H.J. Hovel, "An Isothermal Etchback - Regrowth Method for High Efficiency GaAlAs-GaAs Solar Cells," Appl. Phys. Lett. 30, 492 (1977).
2. R.I. Moon, et al., "Performance of (AlGa)As-GaAs Solar Cells in the Space Environment," 12th IEEE Photovoltaic Specialists Conference, 255 (1975).
3. R.S. Miller and J.S. Harris, "Gallium Arsenide Concentration System," presented at the AIAA Conference on the Future of Aerospace Power System, March 1977.
4. G.H. Walker and E.J. Conway, "Annealing of GaAs Solar Cells Damaged by Electron Irradiation," J. of Electrical Chemical Society, Vol. 125, No. 4, p. 676, 1978.

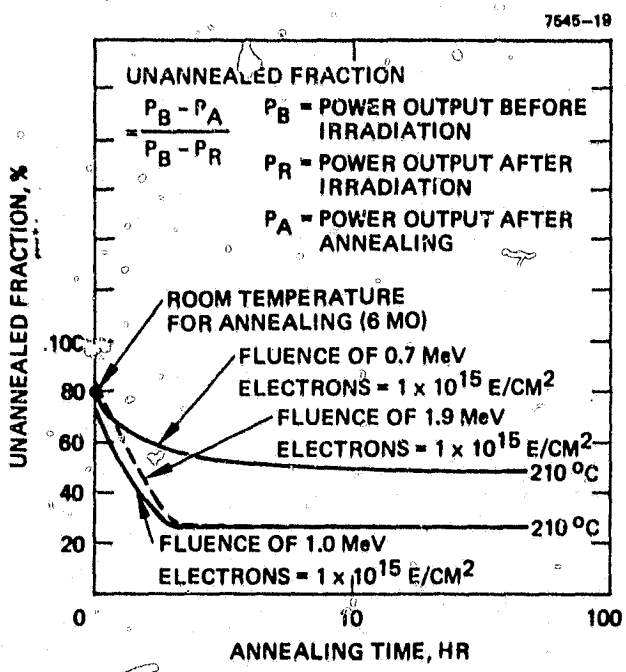

Figure 14. Unannealed fraction versus annealing time

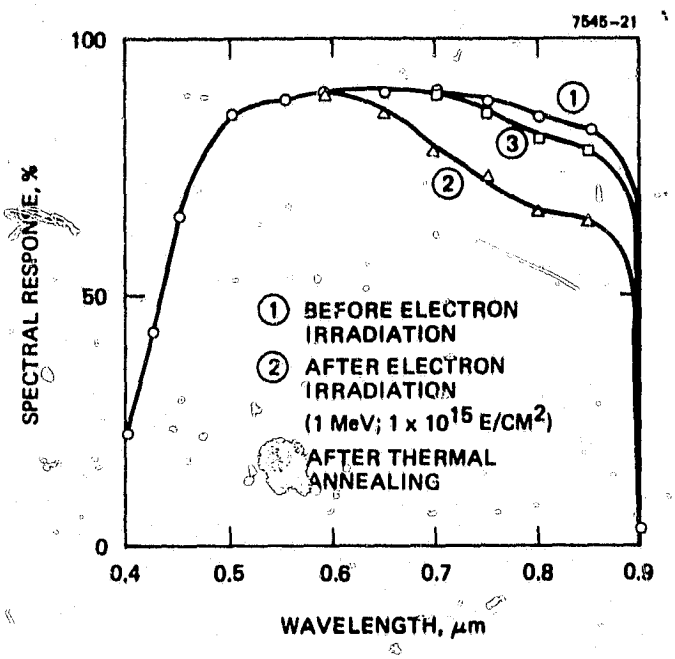

Figure 15(b). Spectral response before and after thermal annealing cell #1008

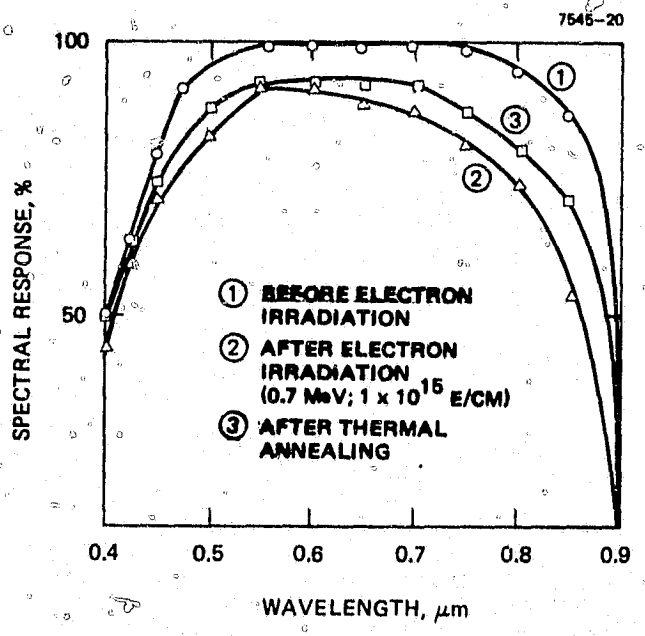

Figure 15(a). Spectral response before and after thermal annealing Cell #1222

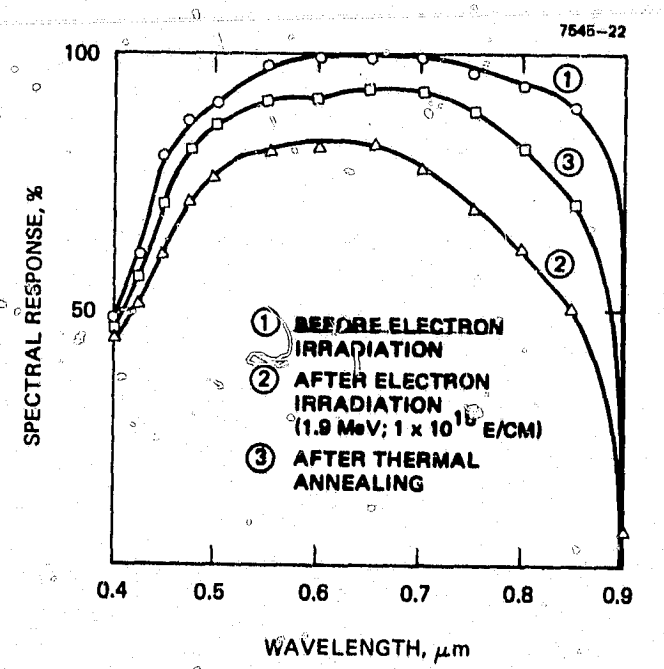

Figure 15(c). Spectral response before and after irradiation and after annealing cell #1278

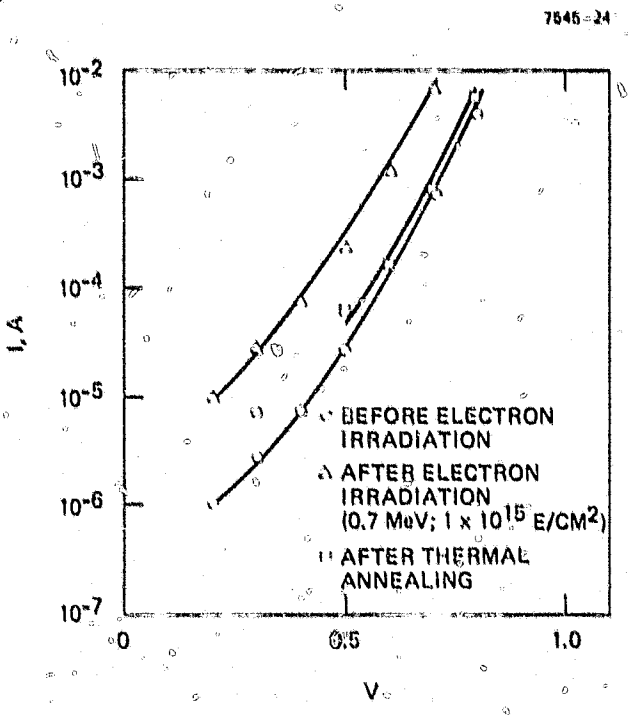

Figure 16(a). Dark I-V characteristic before and after thermal annealing cell #1222

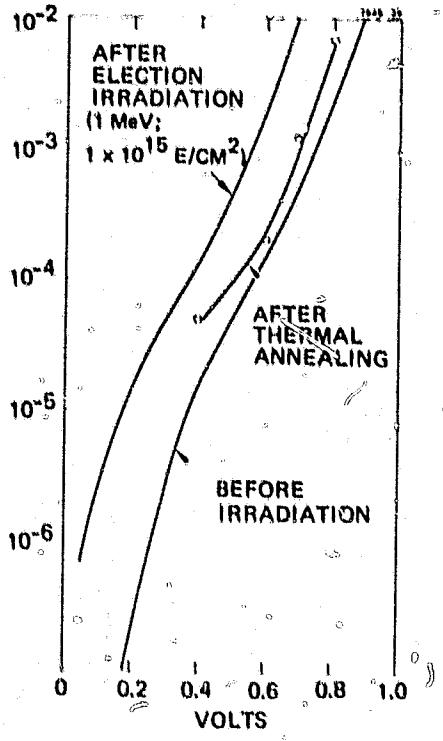

Figure 16(b). Dark I-V characteristic before and after thermal annealing cell #1008

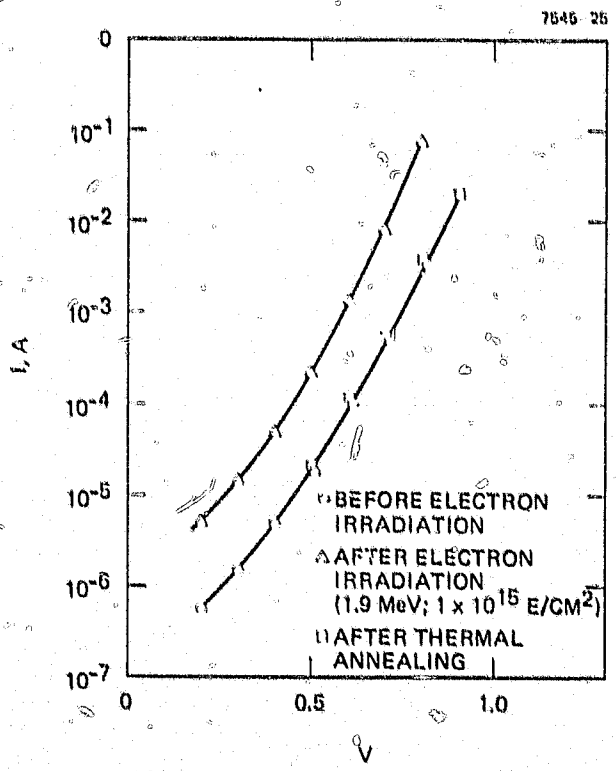

Figure 16(c). Dark I-V characteristic before and after thermal annealing cell #1278

APPENDIX B

PHOTO I-V CHARACTERISTICS OF (AlGa)As-GaAs SOLAR CELL BEFORE AND AFTER 1-MeV ELECTRON IRRADIATION

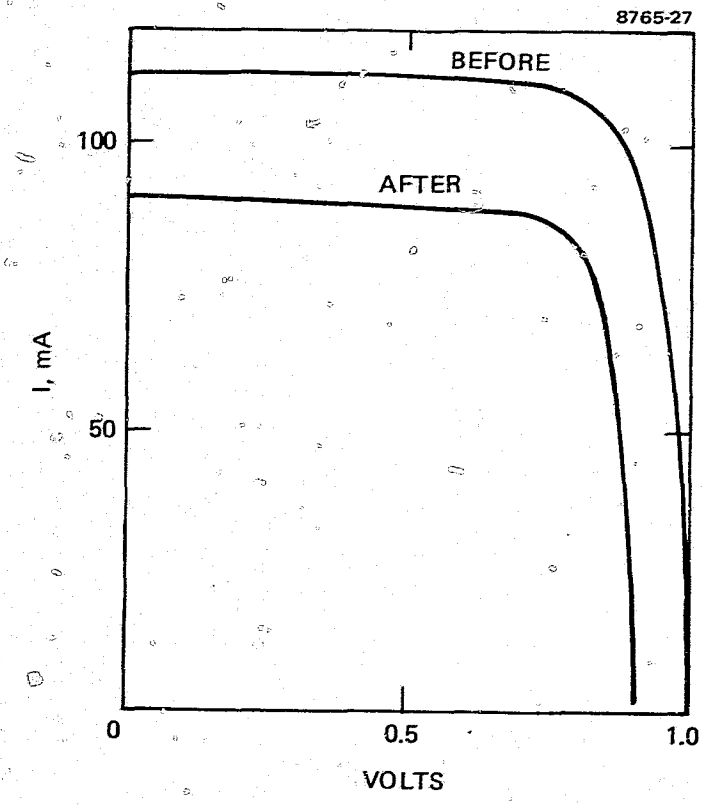

Figure B-1.
Photo I-V characteristics before and after 1-MeV electron irradiation (cell No. 2401, fluence = 1 x 10^{15} e cm^{-2}, irradiation temperature = 28°C).

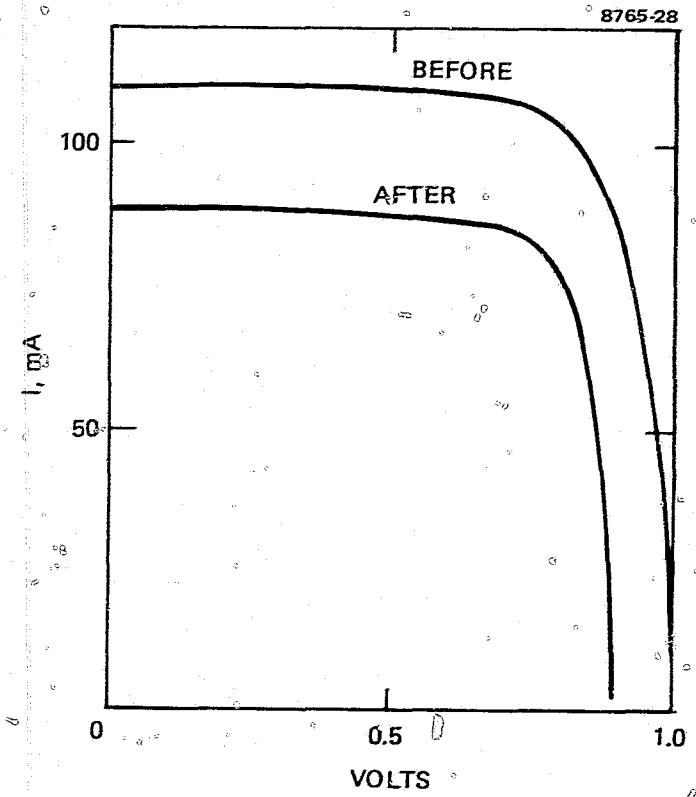

Figure B-2.
Photo I-V characteristics before and after 1-MeV electron irradiation (cell No. 2405, fluence = 1 x 10^{15} e cm^{-2}, irradiation temperature = 28°C).

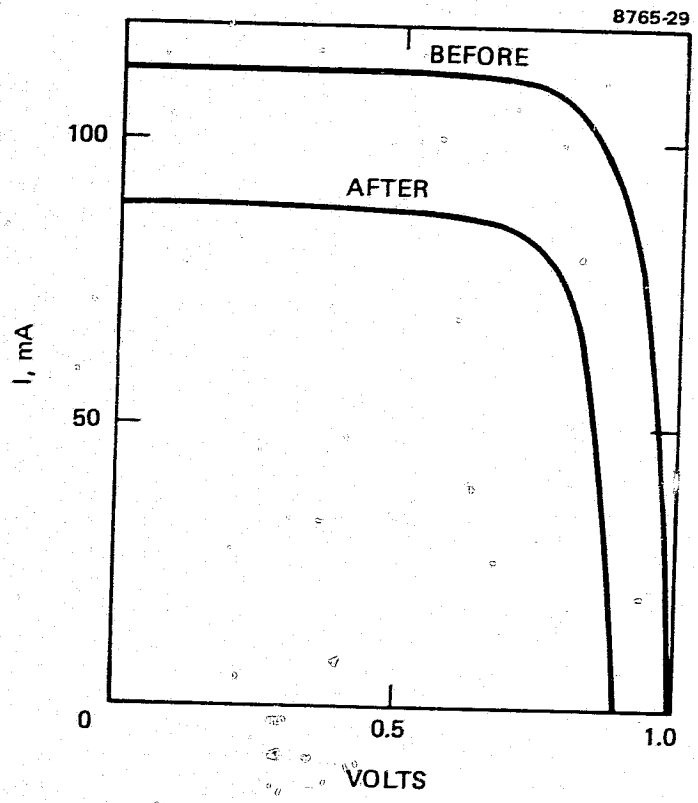

Figure B-3.
Photo I-V characteristics before and after 1-MeV electron irradiation (cell No. 2373, fluence = 1 x 10^{15} e cm^{-2}).

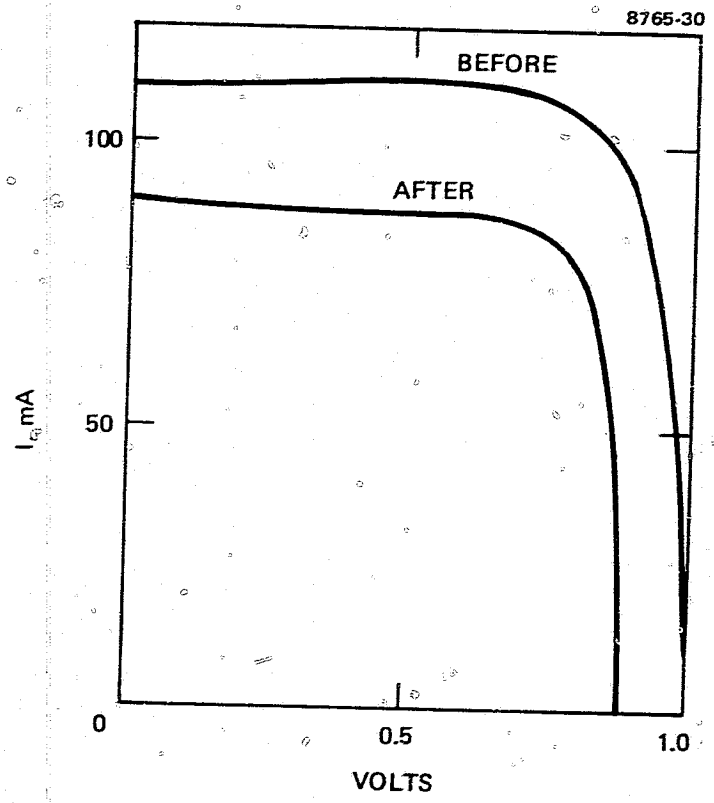

Figure B-4.
Photo I-V characteristics before and after 1-MeV electron irradiation (cell No. 2403, fluence = 1 x 10^{15} e cm^{-2}).

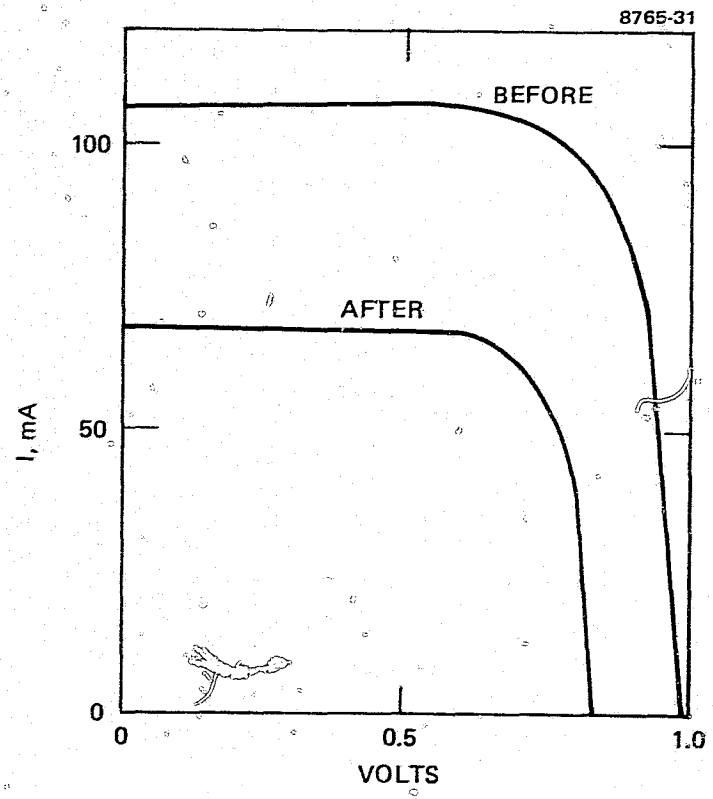

Figure B-5.
Photo I-V characteristics before and after 1-MeV electron irradiation (cell No. 2747, fluence 1 x 10^{16} e cm^{-2}, irradiation temperature = 28°C).

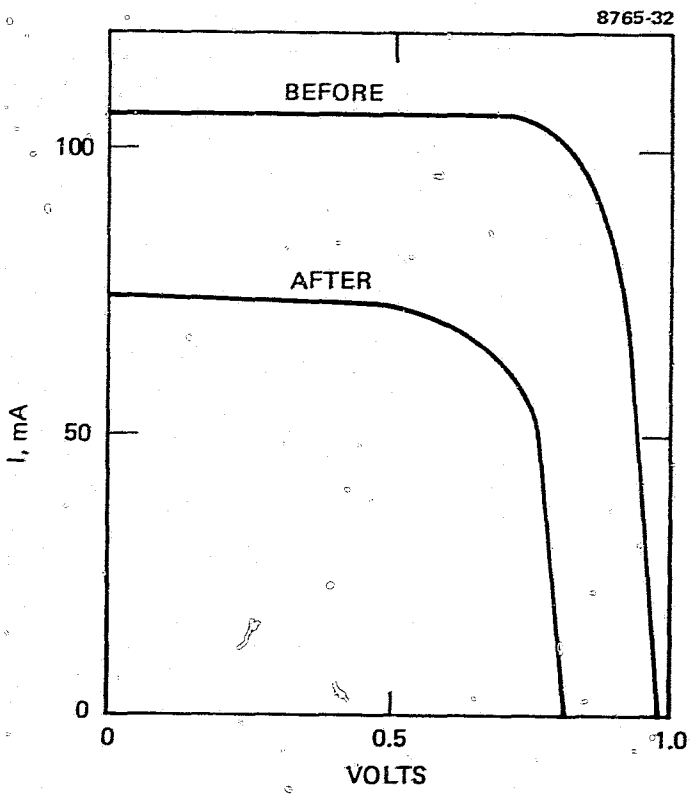

Figure B-6.
Photo I-V characteristics before and after 1-MeV electron irradiation (cell No. 2796, fluence = 1 x 10^{16} e cm^{-2}, irradiation temperature = 28°C).

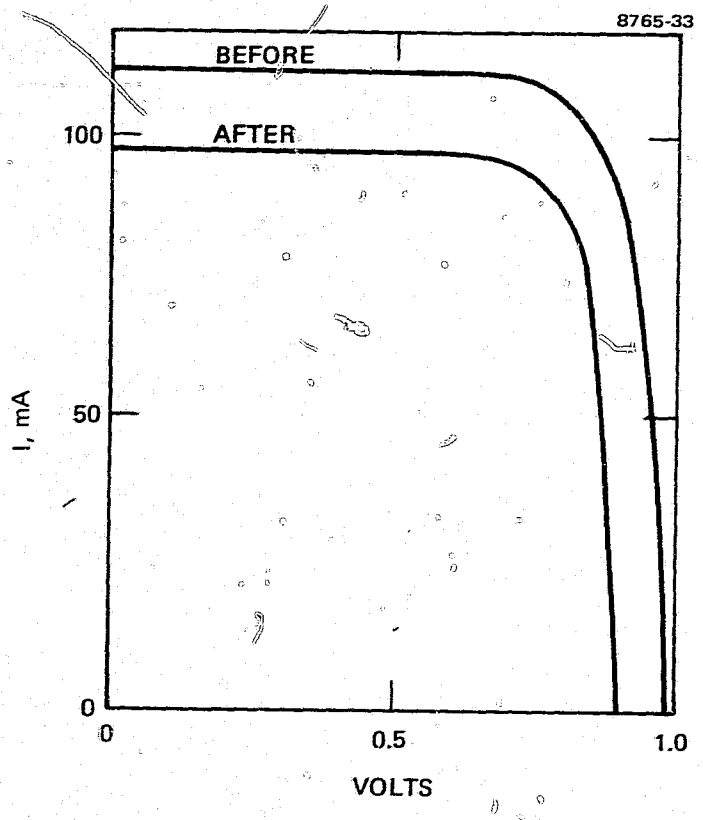

Figure B-7.
Photo I-V characteristics before and after 1-MeV electron irradiation (cell No. 2401, fluence = 1 x 10^{15} e cm^{-2}, irradiation temperature = 28°C).

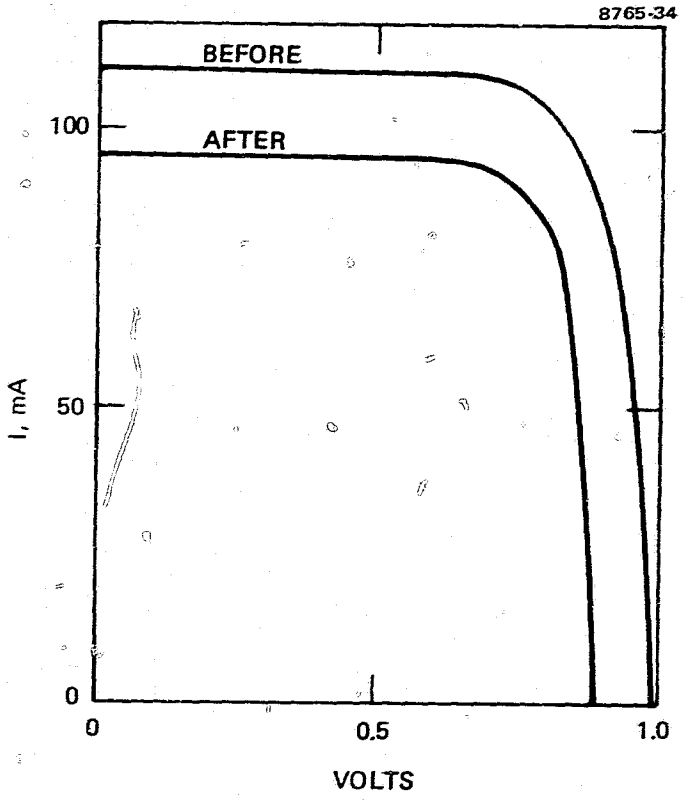

Figure B-8.
Photo I-V characteristics before and after 1-MeV electron irradiation (cell No. 2405, fluence = 1 x 10^{15} e cm^{-2}, irradiation temperature = 28°C).

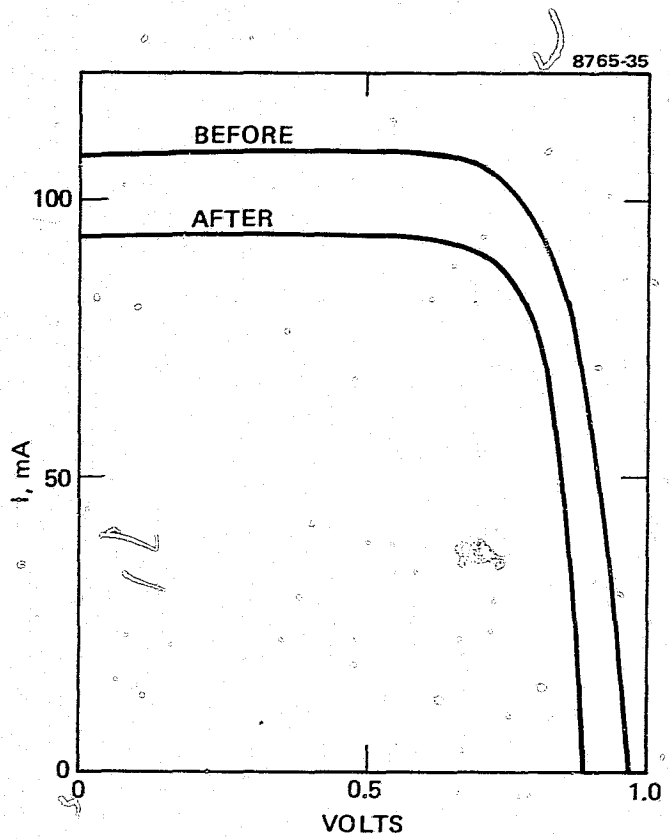

Figure B-9.
Photo I-V characteristics before and after 1-MeV electron irradiation (cell No. 2373, fluence = 1 x 10^{15} e cm^{-2}, irradiation temperature = 126°C.

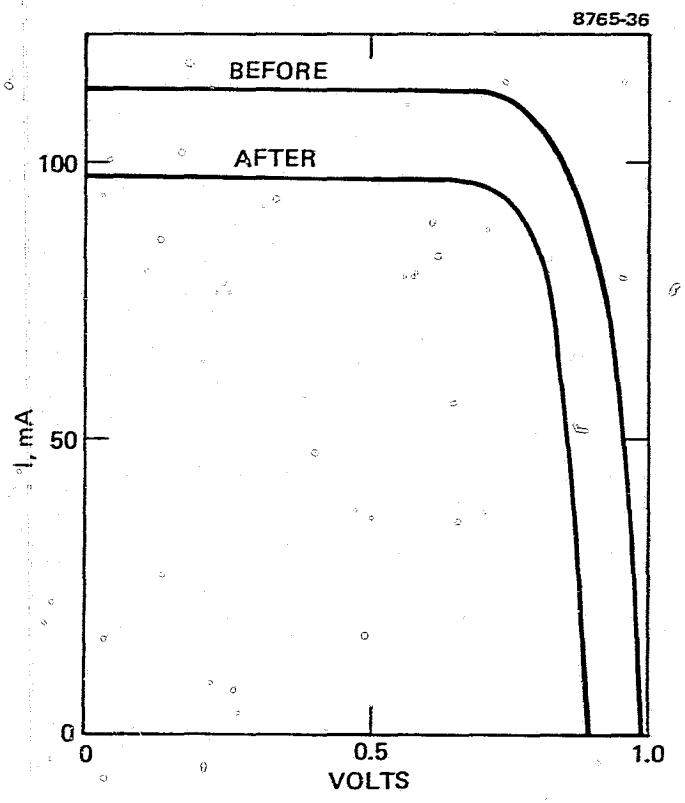

Figure B-10.
Photo I-V characteristics before and after 1-MeV electron irradiation (cell No. 2403, fluence = 1 x 10^{15} e cm^{-2}, irradiation temperature = 126°C).

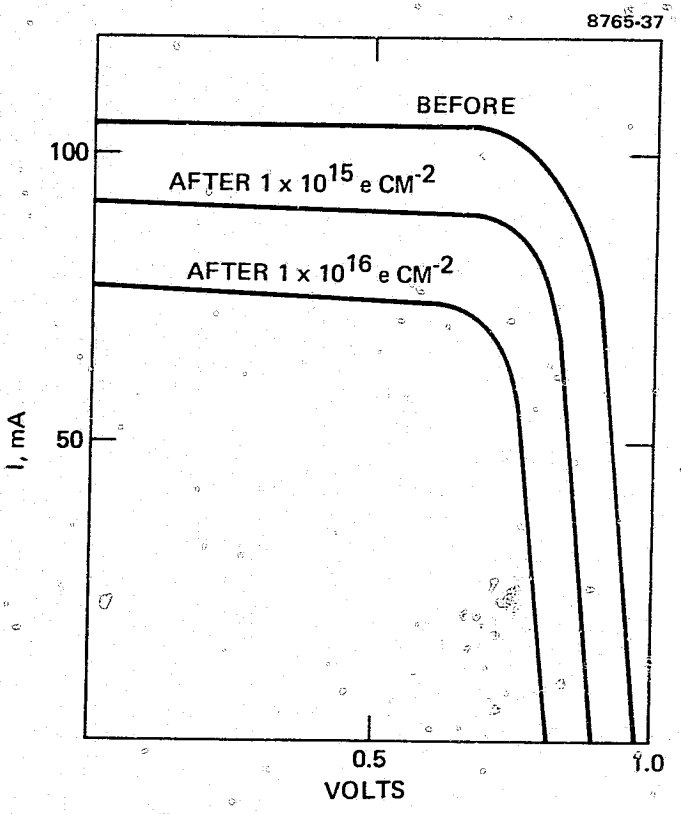

Figure B-11.
Photo I-V characteristics before and after 1-MeV electron irradiation (cell No. 2747, fluence = 1 x 10^{16} e cm^{-2}, irradiation temperature = 28°C).

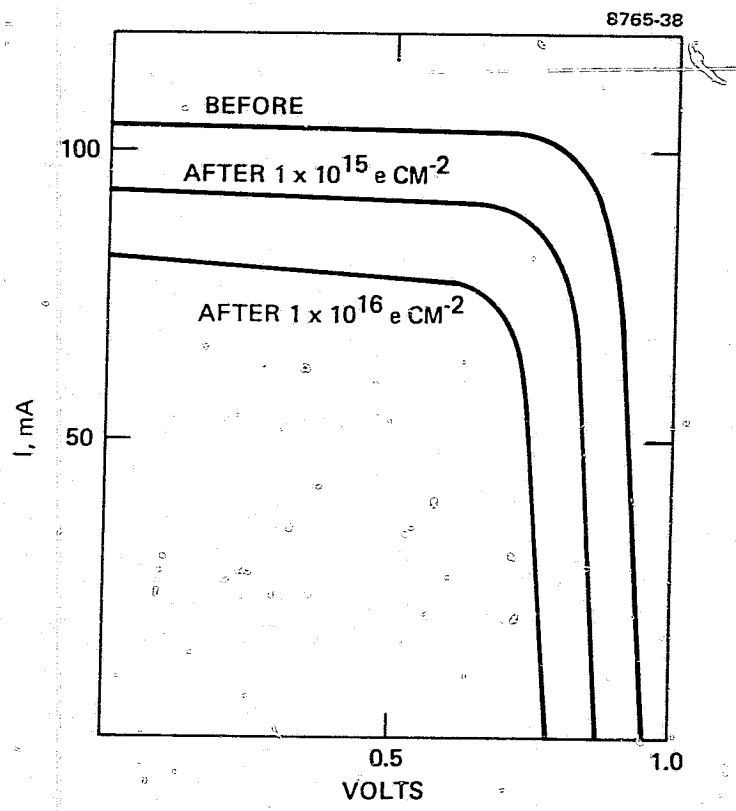

Figure B-12.
Photo I-V characteristics before and after 1-MeV electron irradiation (cell No. 2796, fluence = 1 x 10^{16} e cm^{-2}, irradiation temperature = 28°C).

APPENDIX C

TEMPERATURE MEASUREMENTS ON (AlGa)As-GaAs SOLAR CELLS

The photo I-V characteristics of three (AlGa)As-GaAs solar cells (numbers 2373, 2376, and 2405) were measured in the temperature range between -100 °C and +300°C under vacuum to evaluate their applicability to near-sun missions. Figure C-1 shows the photo I-V characteristics as a function of temperature for cell number 2373. The cell parameters I_{sc}, V_{oc}, and η are plotted versus temperature in Figure C-2. The short-circuit current increases with temperature, and as temperature increases, the open-circuit voltage (V_{oc}) decreases linearly at a rate of about 1.5 mV/°C. This value agrees reasonably with the calculated value of

$$\frac{dV_{oc}}{dT} = 1.7 \text{ mV/°C} ,$$

which was based on the diode leakage current, $I_o(T)$, calculated for the simple diffusion theory. The efficiency decreases with increasing temperature. At above 100°C, η decreases almost linearly at a rate of

$$\frac{\Delta\eta}{\Delta T} = 0.035\%/°C.$$

For reference, our present GaAs cells have an efficiency above 16% (AM0) at 25°C and 9% (AM0) at 300°C. By contrast, silicon cells have a very low efficiency ~7% (AM0) at 120°C and (by extrapolating the data recorded in the JPL solar cell handbook)[1] are virtually unusable at 300°C.

---

[1] Solar Cell Design Handbook JPL SP 43-38, Vol 2 pag. 3.4-3 through 3.4-15, October 1976.

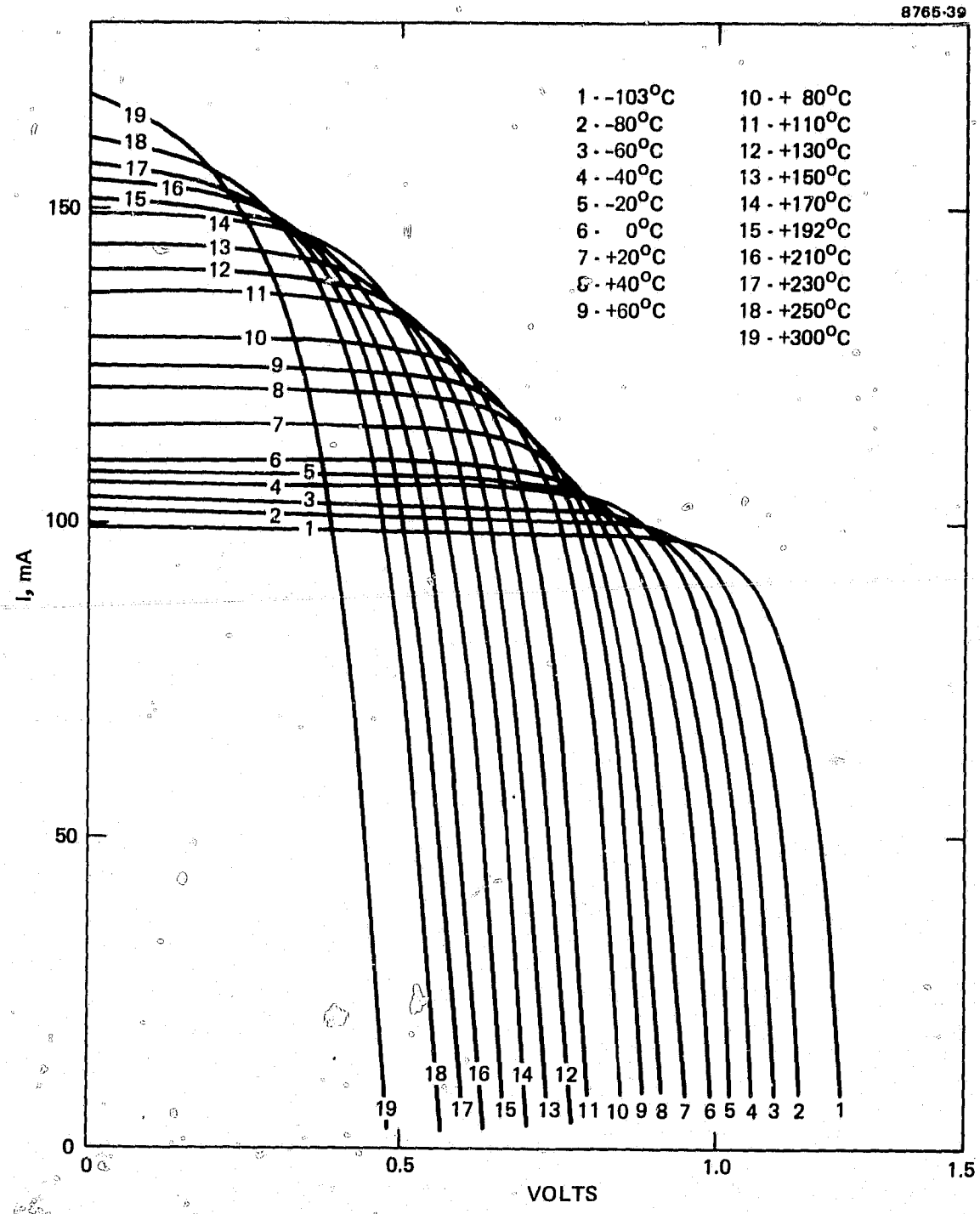

Figure C-1. (AlGa)As-GaAs solar cell photo I-V characteristics as a function of temperature (cell 2373).

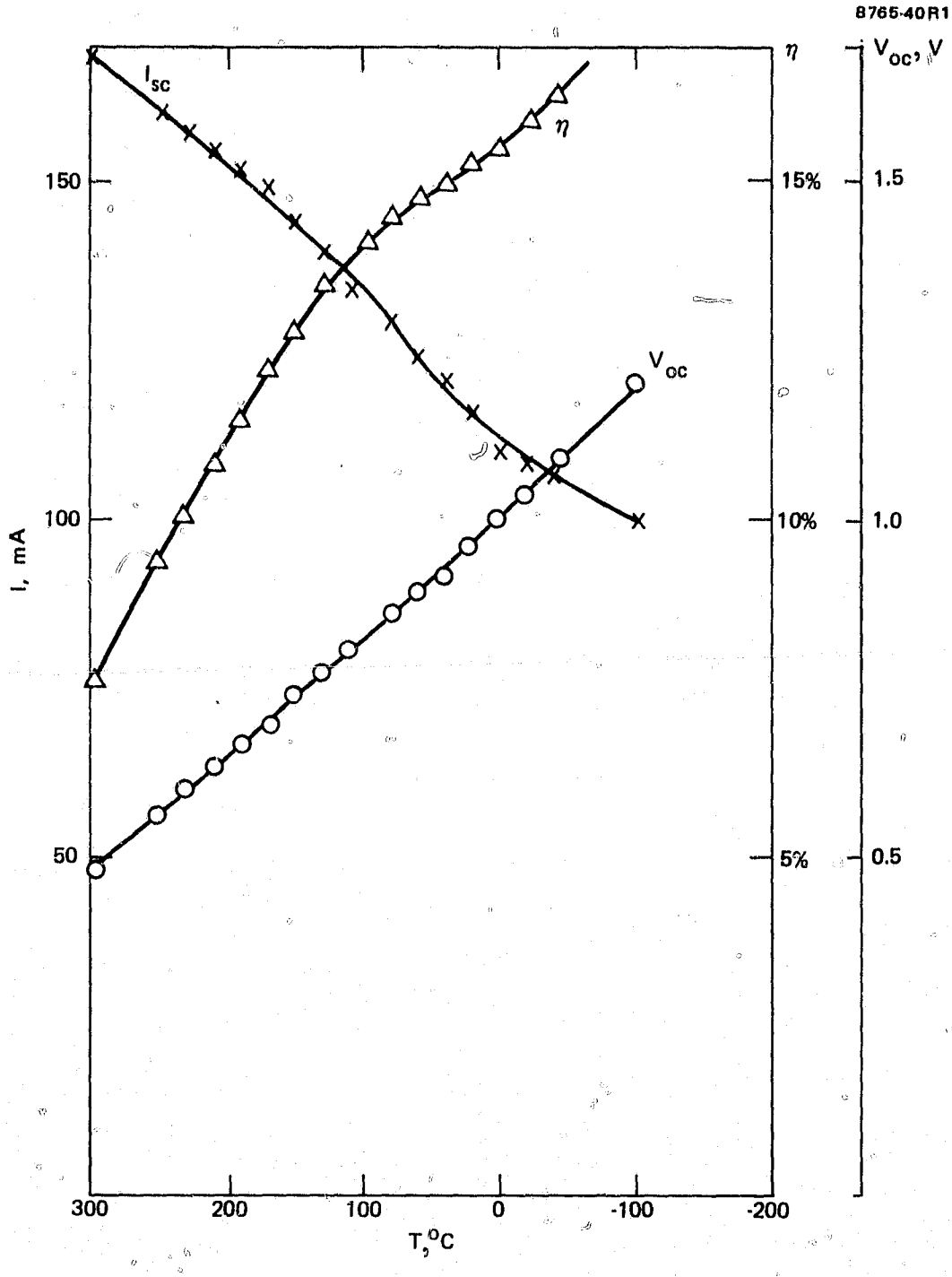

Figure C-2. I_{sc}, V_{oc}, η versus temperature (cell number 2373).